

2D Materials: Properties, Applications and Synthesis Methods

Joan Redwing

4/14/2016

Where is Penn State?



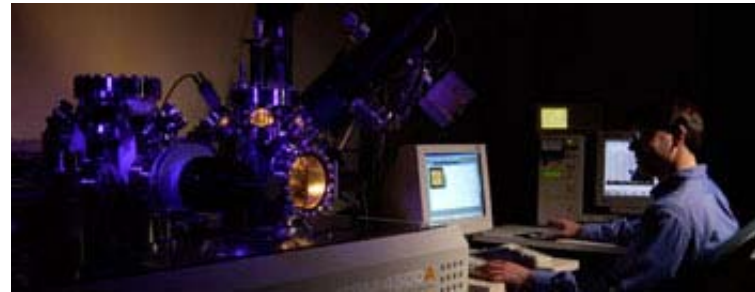
Penn State Information

- Land grant institution, founded in 1855
- Located in State College, Pennsylvania (population~100,000)
- Enrollment ~45,000 students



Materials Research at Penn State

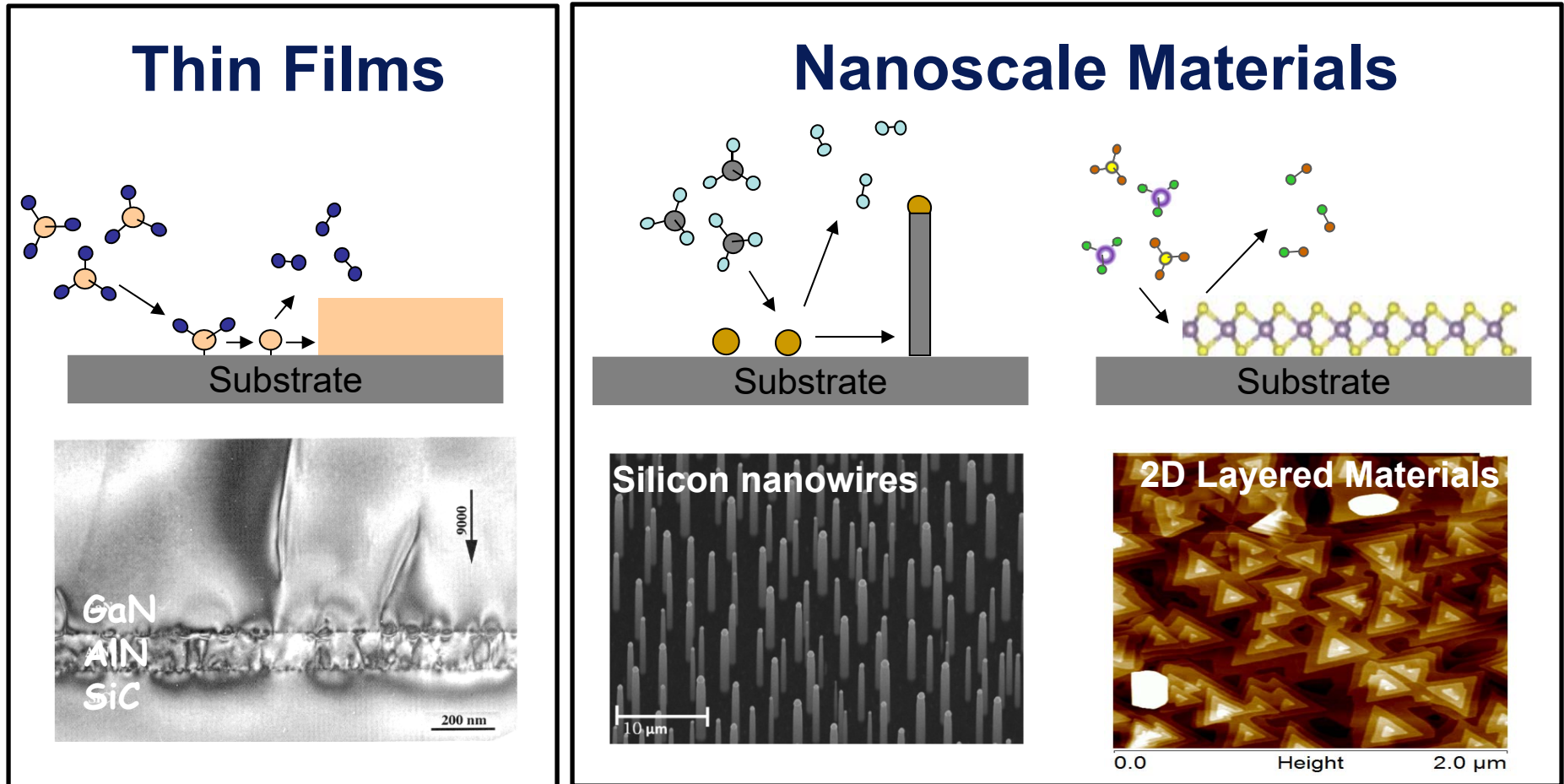
- 200+ faculty, 800+ grad students, 15 academic departments
- Materials Research Institute
- Millennium Science Complex
 - Huck Institute for Life Sciences and Materials Research Institute
 - Nanofabrication Facility (part of National Nanofabrication Infrastructure Network)
 - Materials Characterization Facility



Millennium
Science Complex

Electronic Materials Synthesis

Our research is focused on the development of new processes, materials and device structures using *chemical vapor deposition*-based techniques.



Process Chemistry ↔ Material Structure ↔ Properties ↔ Device Applications



2D Crystal Consortium

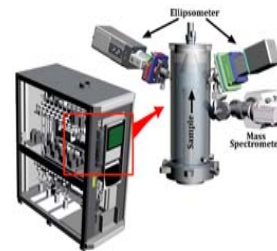
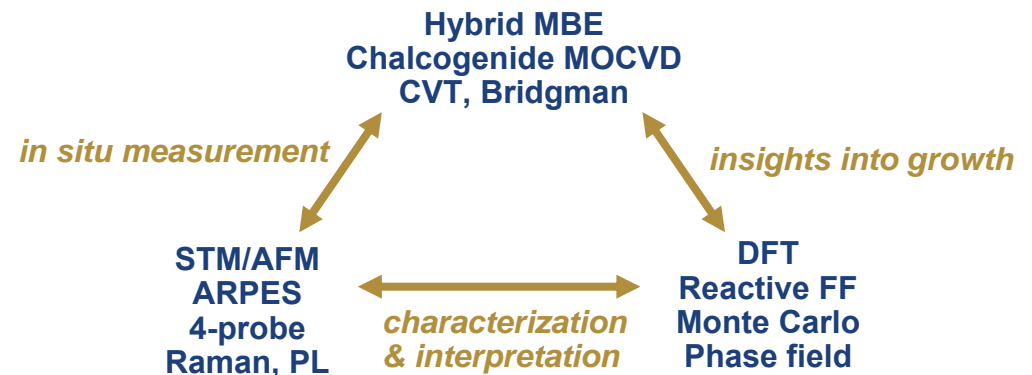
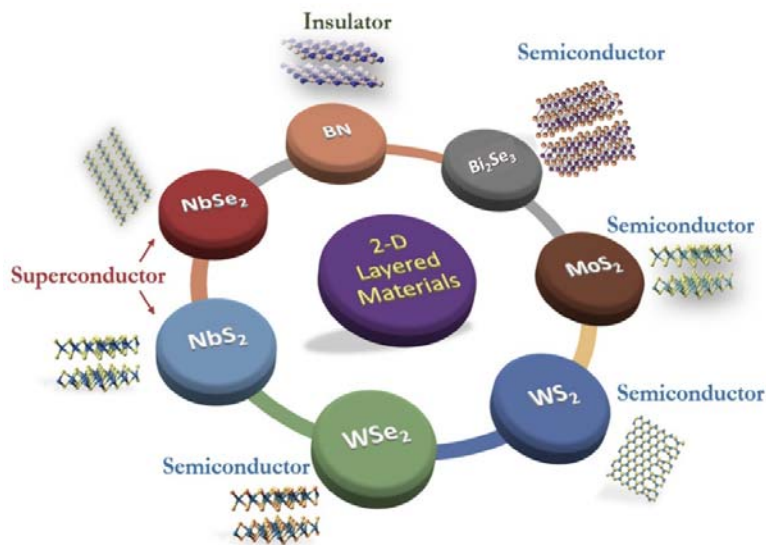
NSF Materials Innovation Platform



PennState

\$17.8M national user facility to advance synthesis of 2D materials for next generation electronics

2D chalcogenide monolayers, surfaces and interfaces are emerging as a compelling class of systems with transformative new science that can be harnessed for novel device technologies in next-generation electronics.



An NSF user facility with broad access:

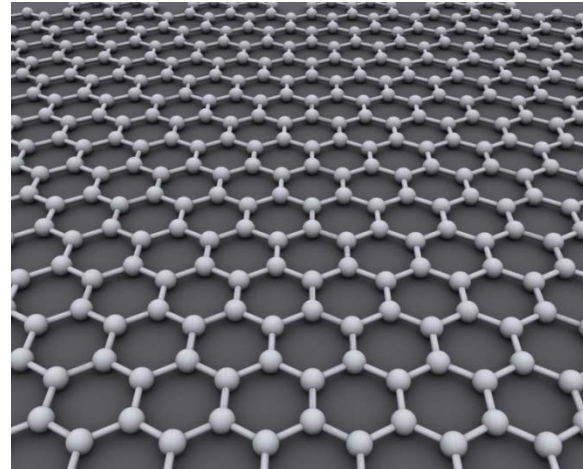
- Open calls for user proposals,
- No user fees for academic use
- Access to a team of local experts
- Community knowledge-base of synthetic protocols

- Webinars, Workshops, Website resources
- Partnership opportunities with PUI, MSI

mip.psu.edu

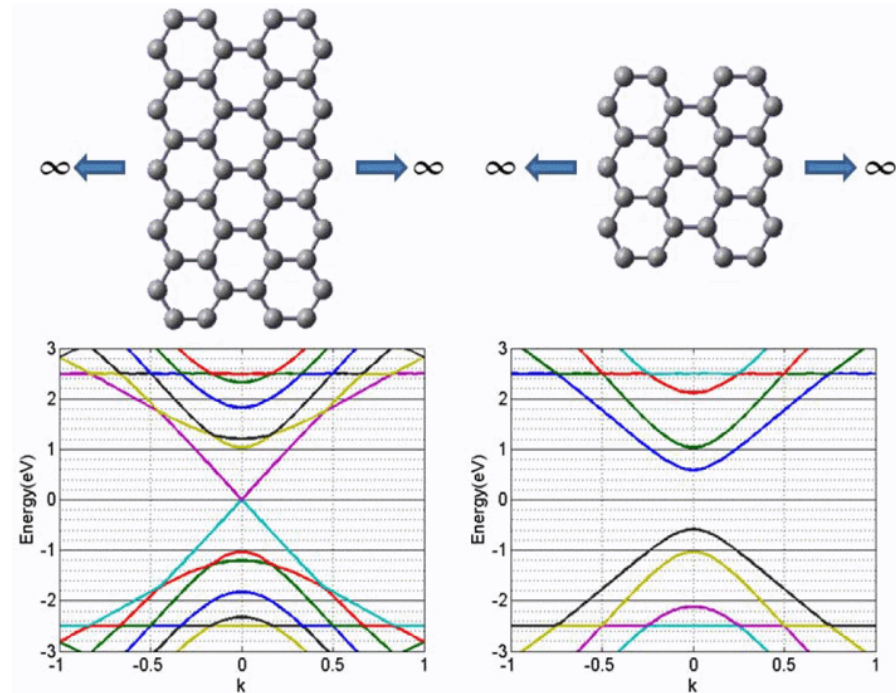
Graphene

- Single layer of carbon atoms



Properties:

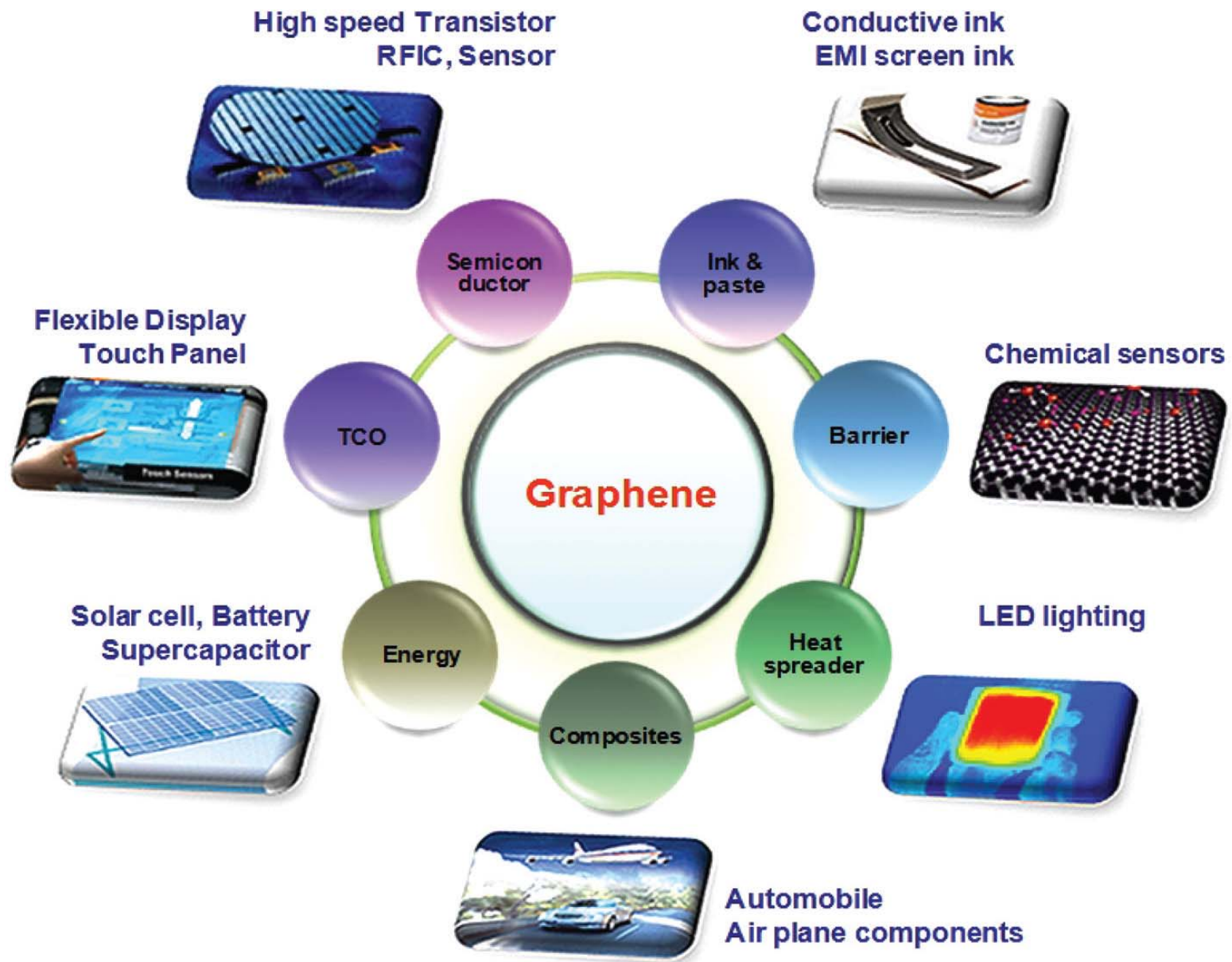
- Mechanically strong
- Flexible
- Optically transparent
- Good conductor of heat and current
- Semi-metal
- Graphene nanoribbons are semiconducting



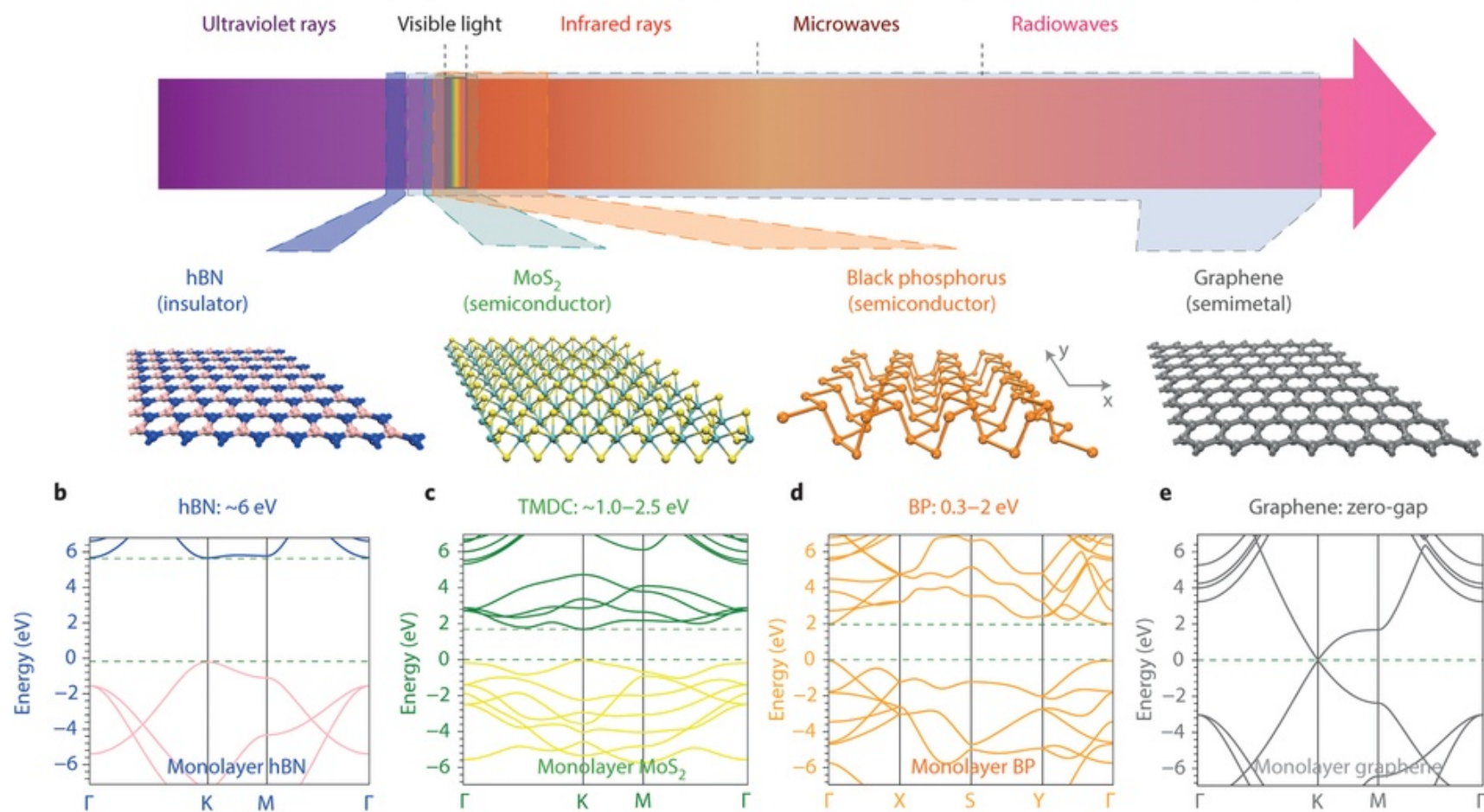
Graphene
(semi-metal)

Graphene nanoribbon
(semiconductor)

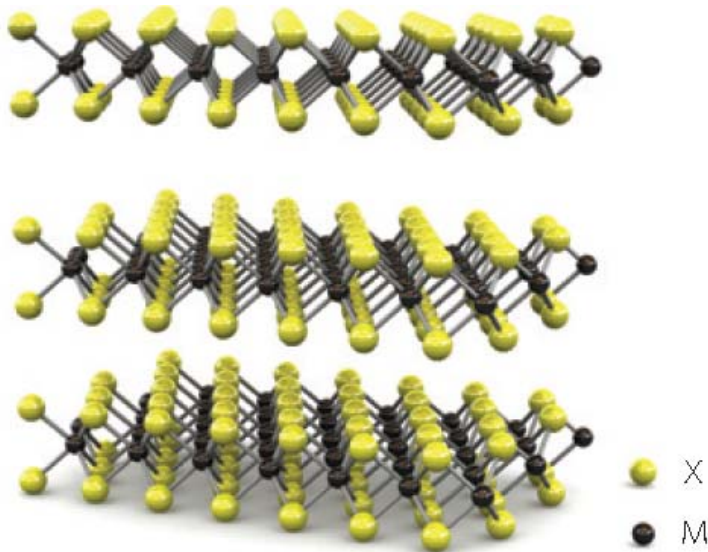
Applications for Graphene



Beyond Graphene....



2D Chalcogenides



- Graphene-like layered materials
- Exhibit wide variety of electronic properties – insulators, semiconductors, metals, superconductors

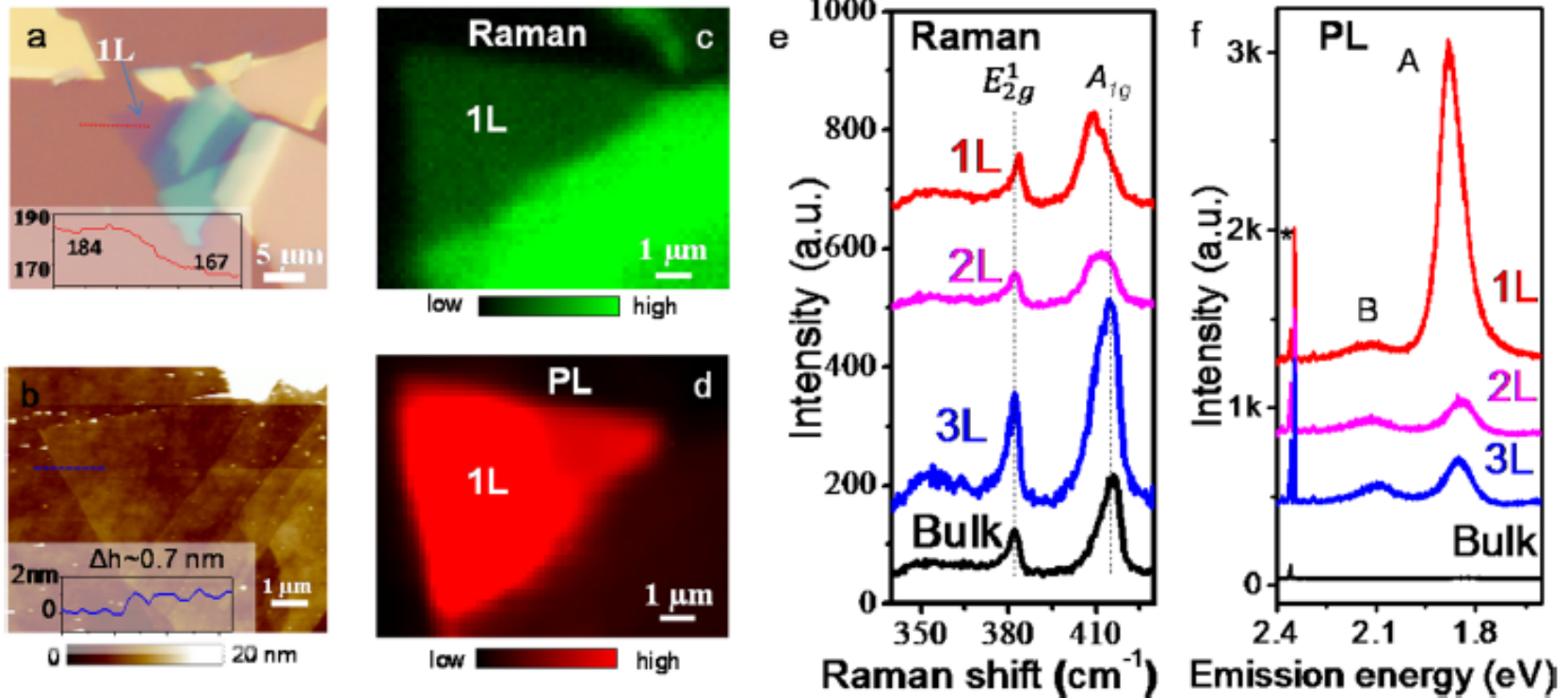
*Q.H. Huang, et al.
Nature Nanotech. 7 (2012) p. 699*

Graphene family	Graphene	hBN 'white graphene'	BCN	Fluorographene	Graphene oxide
2D chalcogenides	MoS ₂ , WS ₂ , MoSe ₂ , WSe ₂		Semiconducting dichalcogenides: MoTe ₂ , WTe ₂ , ZrS ₂ , ZrSe ₂ and so on	Metallic dichalcogenides: NbSe ₂ , NbS ₂ , TaS ₂ , TiS ₂ , NiSe ₂ and so on	
				Layered semiconductors: GaSe, GaTe, InSe, Bi ₂ Se ₃ and so on	

*A.K. Geim and I.V. Grigorieva
Nature 499 (2013) p. 419*

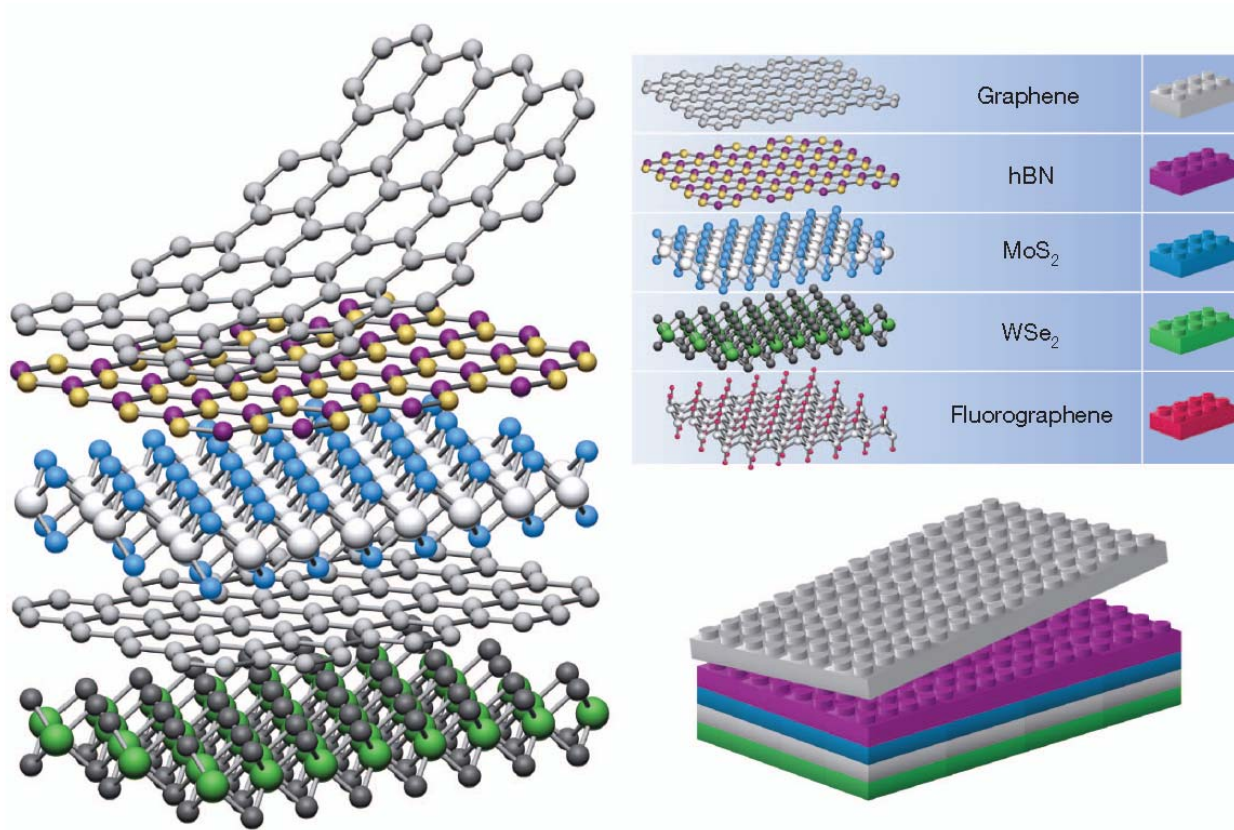
Thickness-Dependent Properties

- Dramatic changes in optical and electronic properties as material is thinned from bulk to a monolayer (1 layer)
 - in-direct bandgap to direct bandgap semiconductor
 - Changes in symmetry – alters polarization



Y.F. Chen, et al.
ACS Nano 7 (2013) 4610-4616.

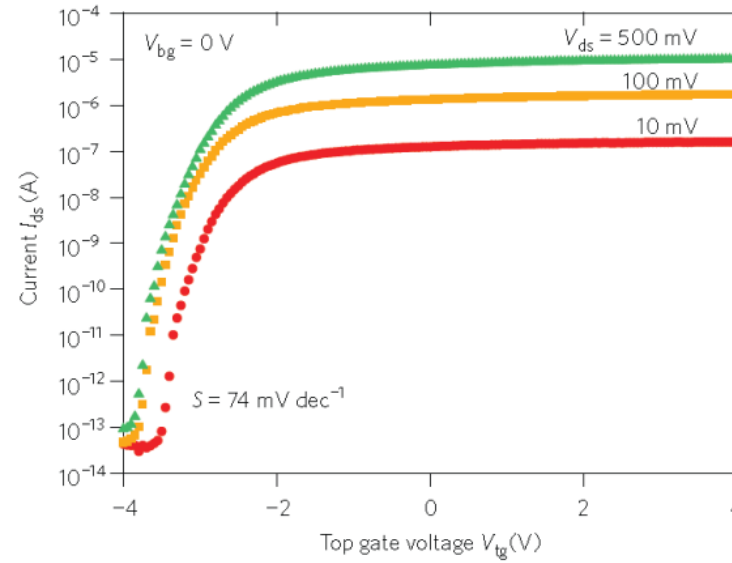
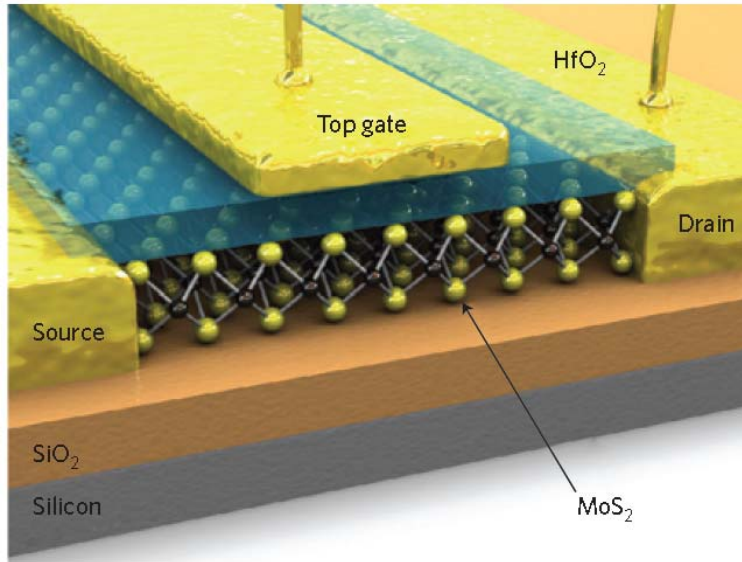
2D Heterostructures



*A.K. Geim and I.V. Grigorieva
Nature 499 (2013) p. 419*

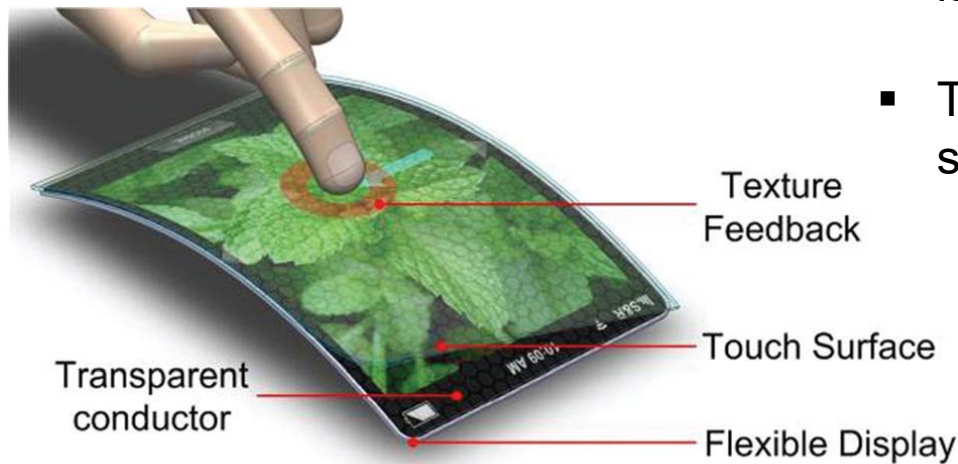
- Van der Waals bonding enables stacking of different materials without need to form chemical bonds

2D Electronics



Q.H. Huang, et al.
Nature Nanotech. 7 (2012) p. 699

- Transistors made of atomically thin layers (good for electrostatics)
- Transfer of 2D layers onto plastic substrates for flexible electronics



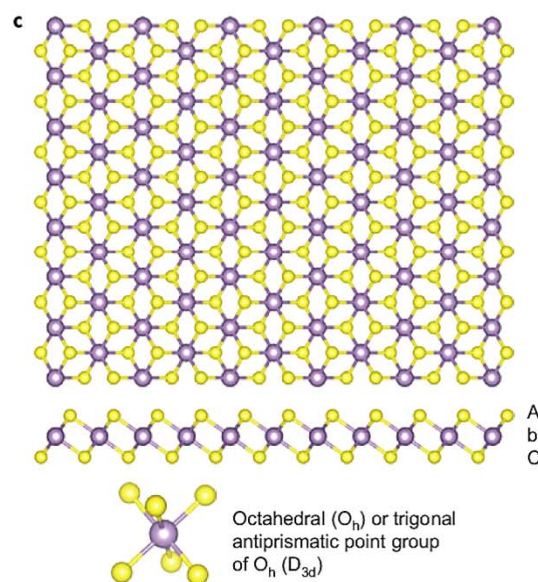
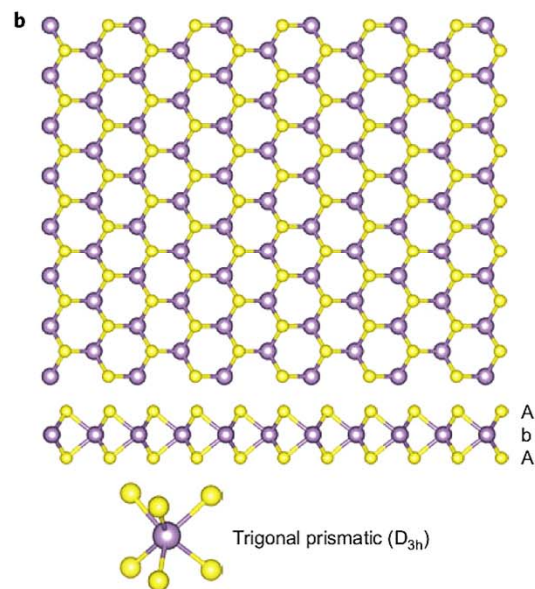
The chemistry of two-dimensional layered transition metal dichalcogenide nanosheets

Manish Chhowalla^{1*}, Hyeon Suk Shin², Goki Eda^{3,4,5}, Lain-Jong Li⁶, Kian Ping Loh^{4,5} and Hua Zhang⁷

a

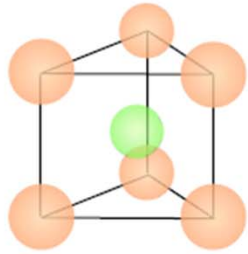
MX₂
M = Transition metal
X = Chalcogen

H																	He
Li	Be											B	C	N	O	F	Ne
Na	Mg	3	4	5	6	7	8	9	10	11	12	Al	Si	P	S	Cl	Ar
K	Ca	Sc	Ti	V	Cr	Mn	Fe	Co	Ni	Cu	Zn	Ga	Ge	As	Se	Br	Kr
Rb	Sr	Y	Zr	Nb	Mo	Tc	Ru	Rh	Pd	Ag	Cd	In	Sn	Sb	Te	I	Xe
Cs	Ba	La-Lu	Hf	Ta	W	Re	Os	Ir	Pt	Au	Hg	Tl	Pb	Bi	Po	At	Rn
Fr	Ra	Ac-Lr	Rf	Db	Sg	Bh	Hs	Mt	Ds	Rg	Cn	Uut	Fl	Uup	Lv	Uus	Uuo



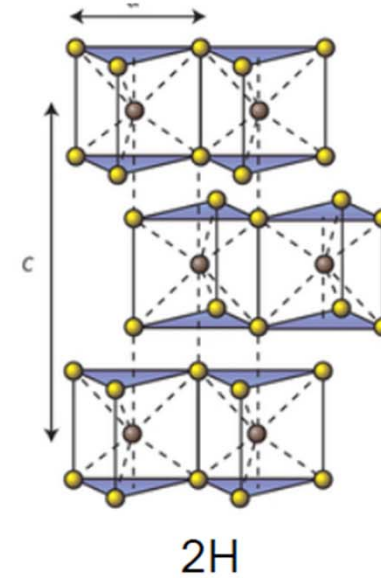
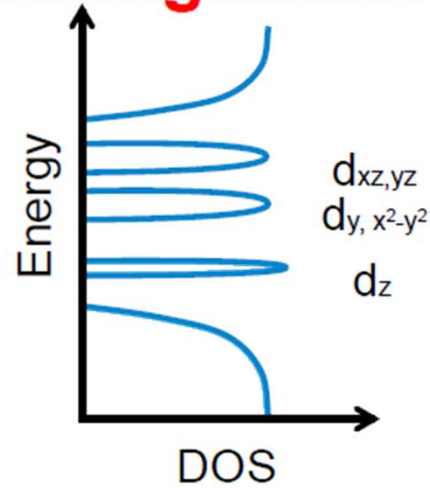
Most Common Structures of TMDs

- semiconductor

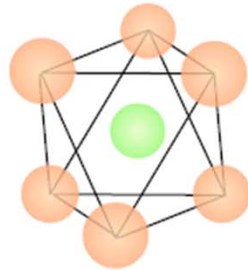


Trigonal prismatic (2H)

2H configuration

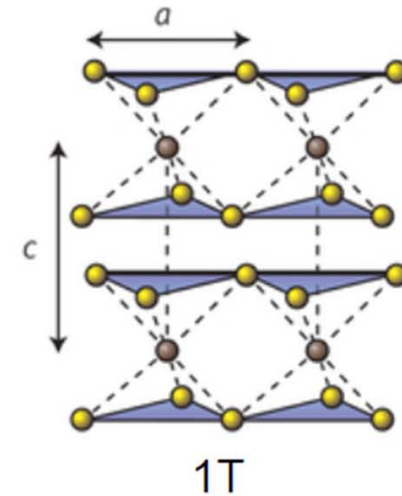
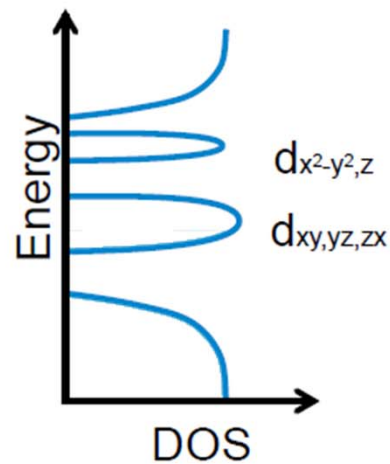


- semimetal



Octahedral (1T)

1T configuration



Electronic character of 2D chalcogenides

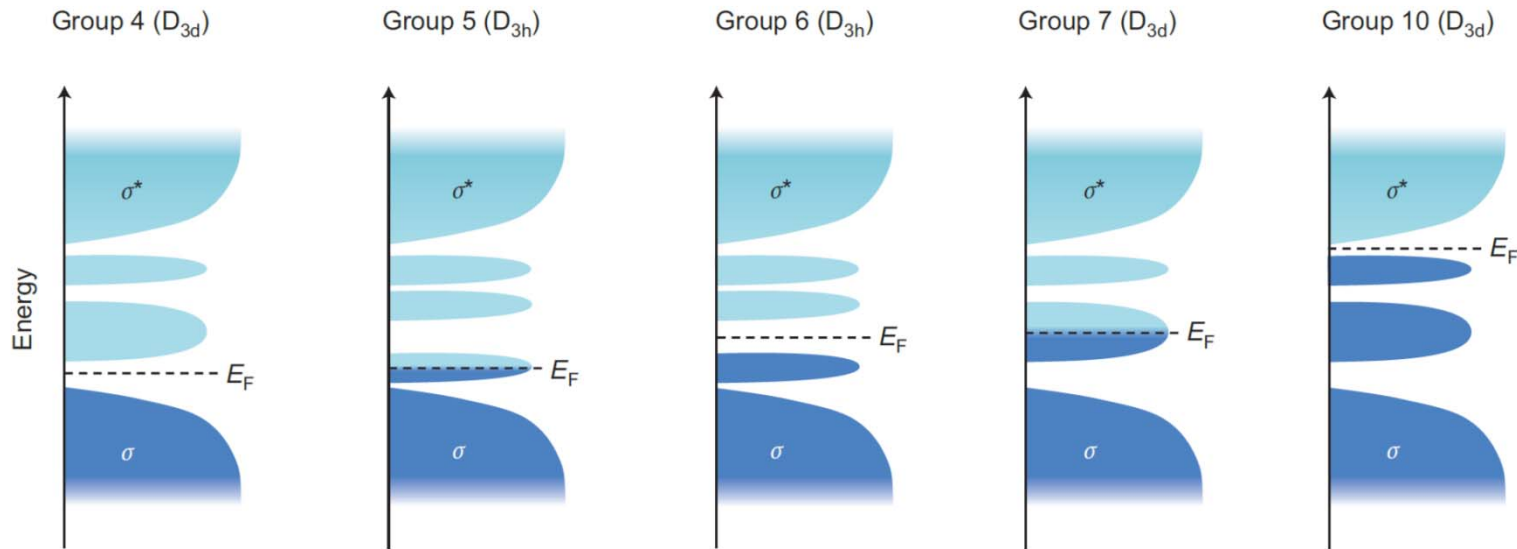
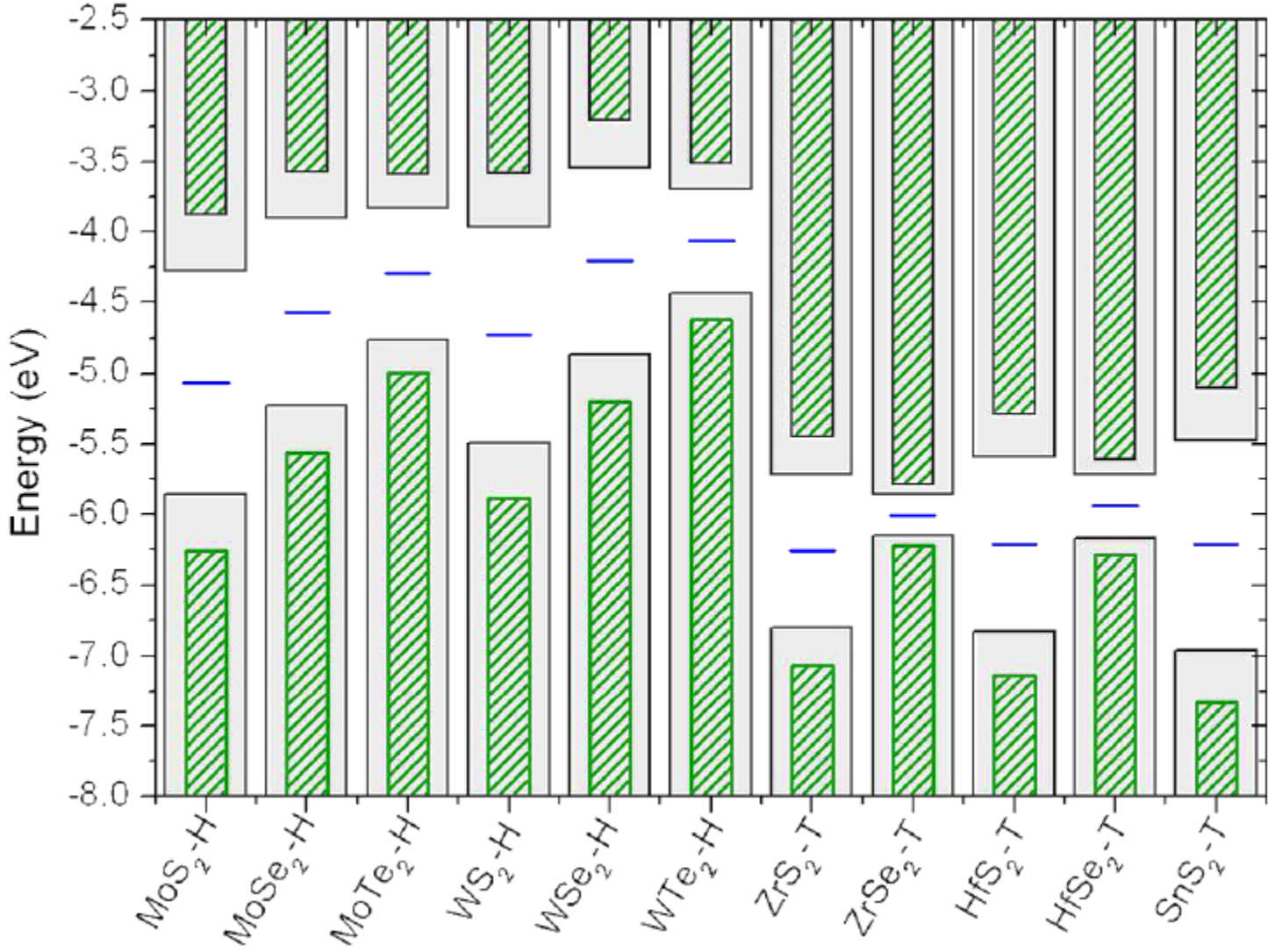


Table 1 | Electronic character of different layered TMDs²⁵.

Group	M	X	Properties
4	Ti, Hf, Zr	S, Se, Te	Semiconducting ($E_g = 0.2\text{-}2\text{ eV}$). Diamagnetic.
5	V, Nb, Ta	S, Se, Te	Narrow band metals ($\rho \sim 10^{-4}\ \Omega\cdot\text{cm}$) or semimetals. Superconducting. Charge density wave (CDW). Paramagnetic, antiferromagnetic, or diamagnetic.
6	Mo, W	S, Se, Te	Sulfides and selenides are semiconducting ($E_g \sim 1\text{ eV}$). Tellurides are semimetallic ($\rho \sim 10^{-3}\ \Omega\ \text{cm}$). Diamagnetic.
7	Tc, Re	S, Se, Te	Small-gap semiconductors. Diamagnetic.
10	Pd, Pt	S, Se, Te	Sulfides and selenides are semiconducting ($E_g = 0.4\text{ eV}$) and diamagnetic. Tellurides are metallic and paramagnetic. PdTe_2 is superconducting.

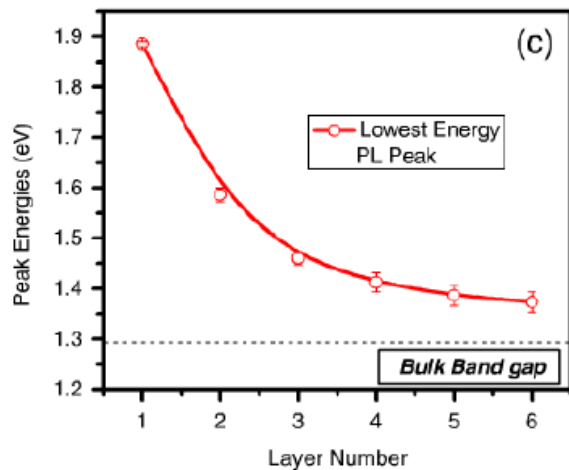
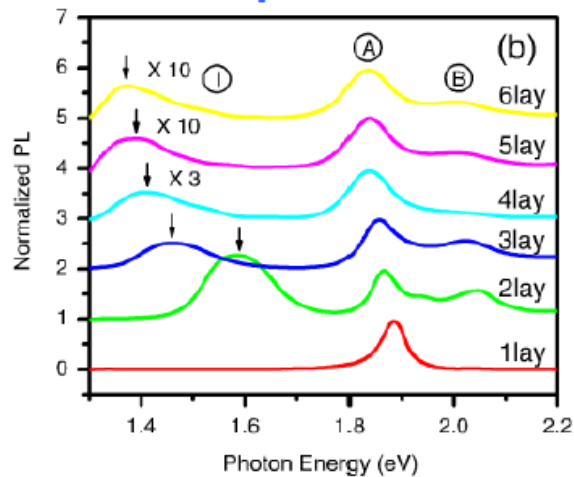
ρ , in-plane electrical resistivity.

Band alignment of layered chalcogenides

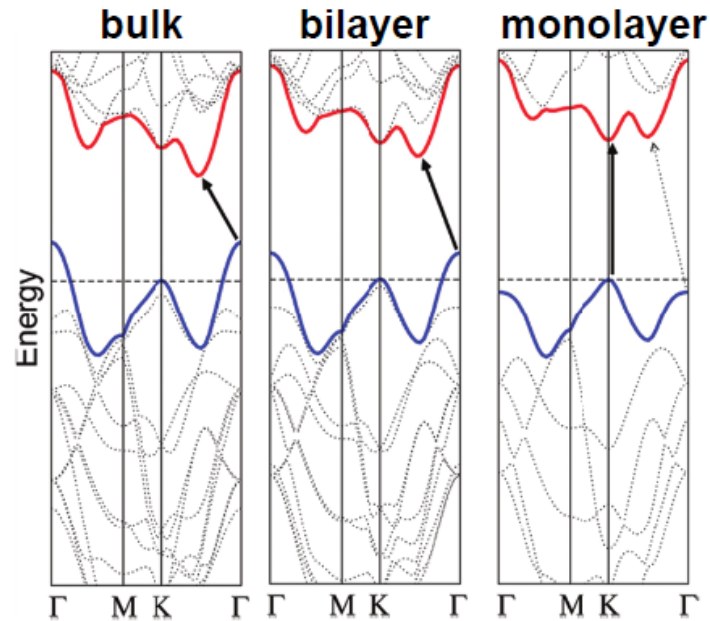


From Monolayer to Bulk: Photoluminescence Change

Photoluminescence spectra



Energy band structure



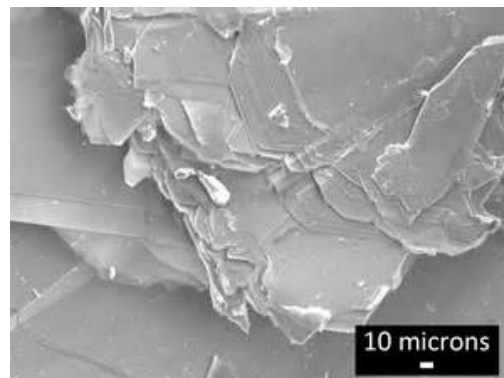
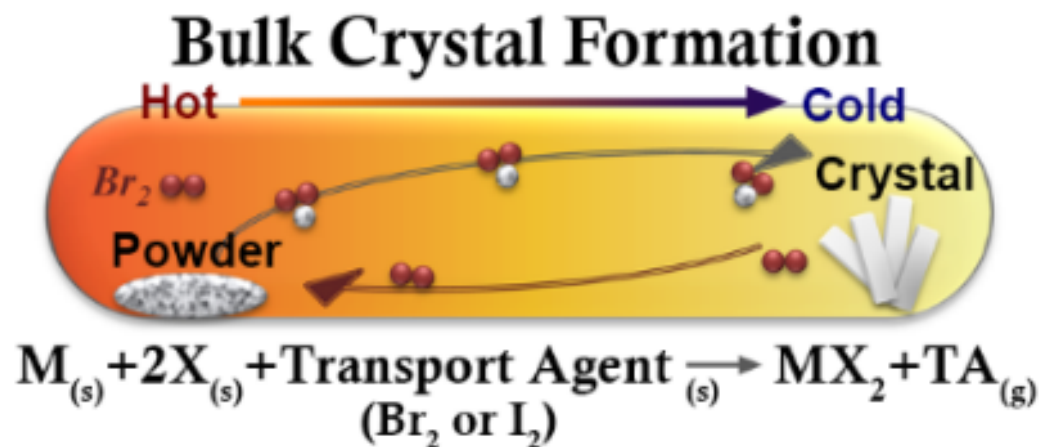
Nano Lett. 10:1271-1275 (2010)

- With increasing number of layers, the photoluminescence intensity decreases, due to energy band changes
- Monolayer MoS₂: direct bandgap
- Bilayer or thicker MoS₂: indirect bandgap
- This suggests strong interlayer interaction

ATE

Bulk 2D chalcogenides (MoS₂ example)

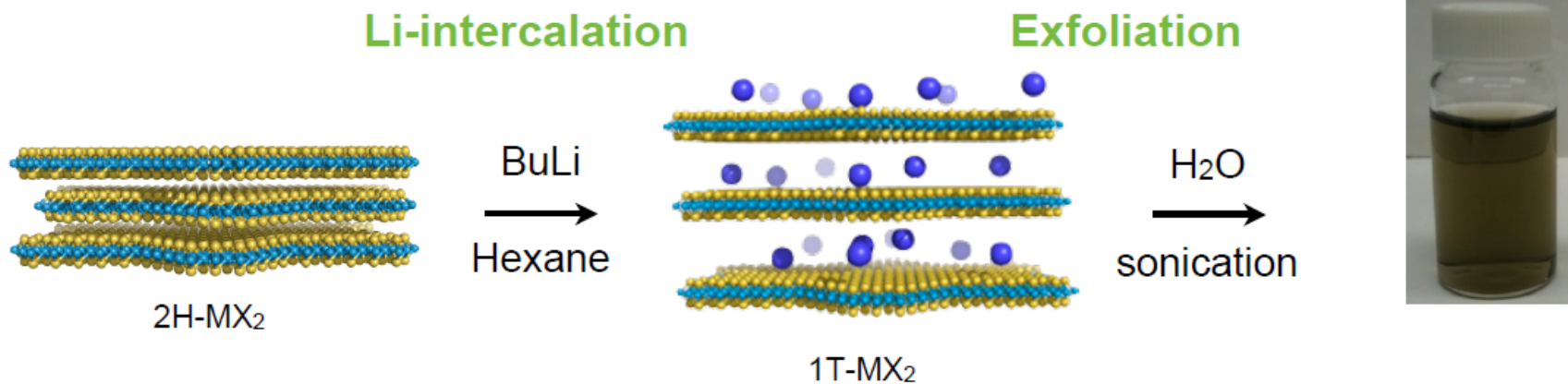
- Naturally occurring in molybdenite ore
 - Powder used in lubricants
- Bulk synthesis methods (for higher purity material):
 - Sulfurization of MoO₃ powder (Heat in H₂S, etc.)
 - Chemical vapor transport



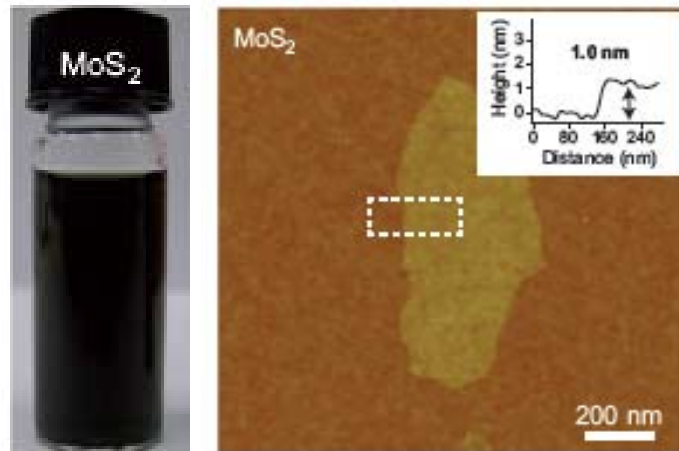
Manchester
Nanocrystals

Chemical exfoliation of TMDs (MX_2)

Mechanism of exfoliation

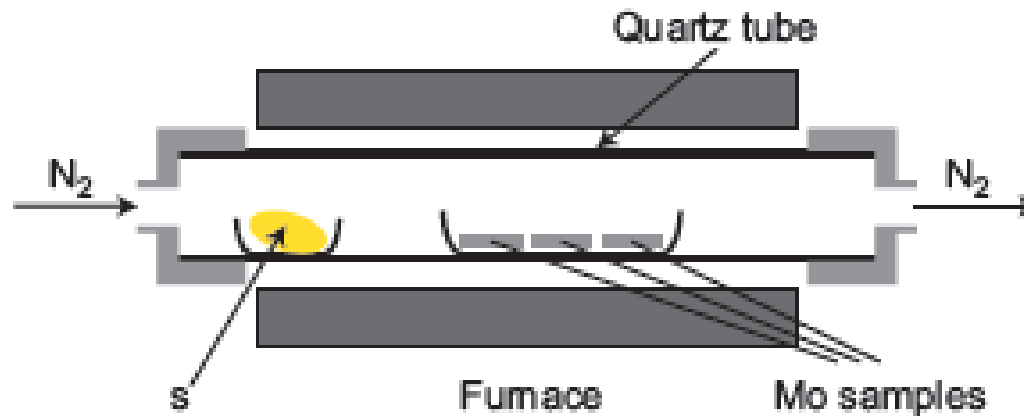


Joensen, Frindt, Morrison, **Single-layer MoS₂**. Mater. Res. Bull. (1986).

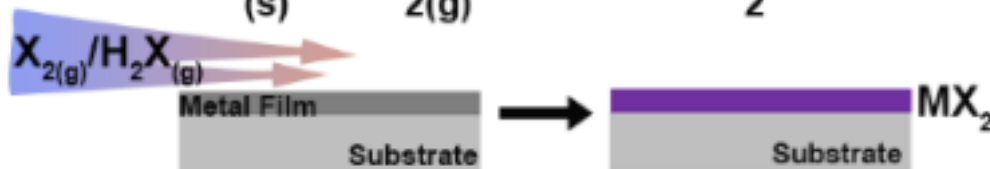
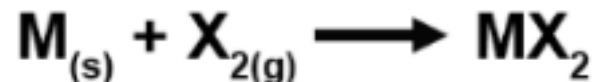


M. Chhowalla, et al.
Nature Chemistry 5 (2013) p. 264

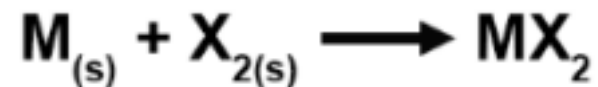
Metal transformation



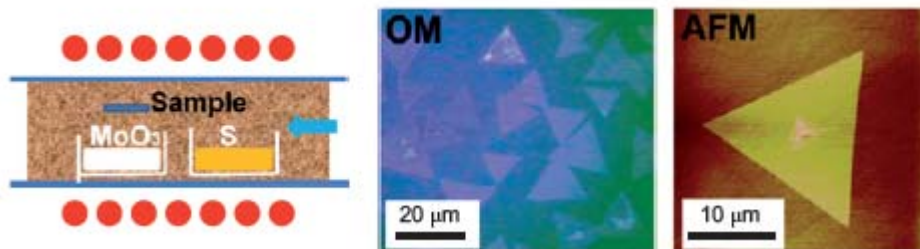
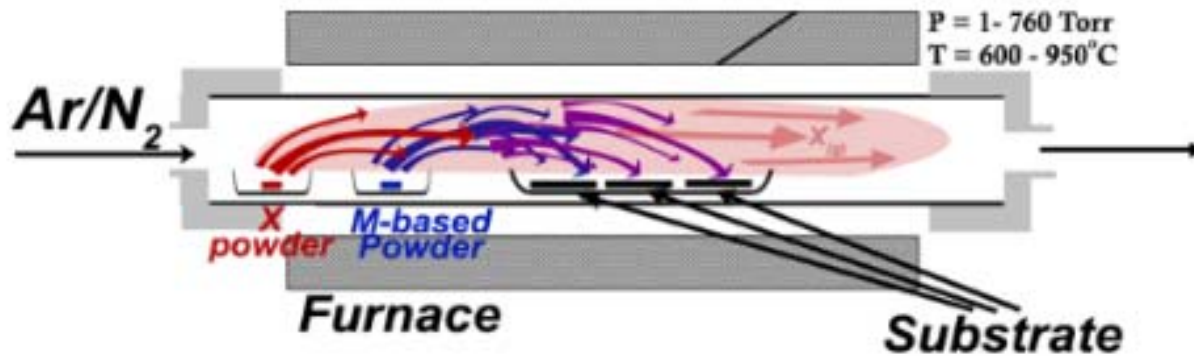
"Soft Chalcogenization"



Solid State Reactions



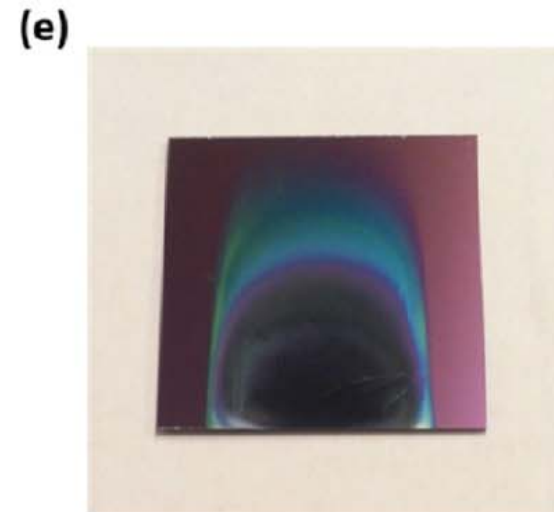
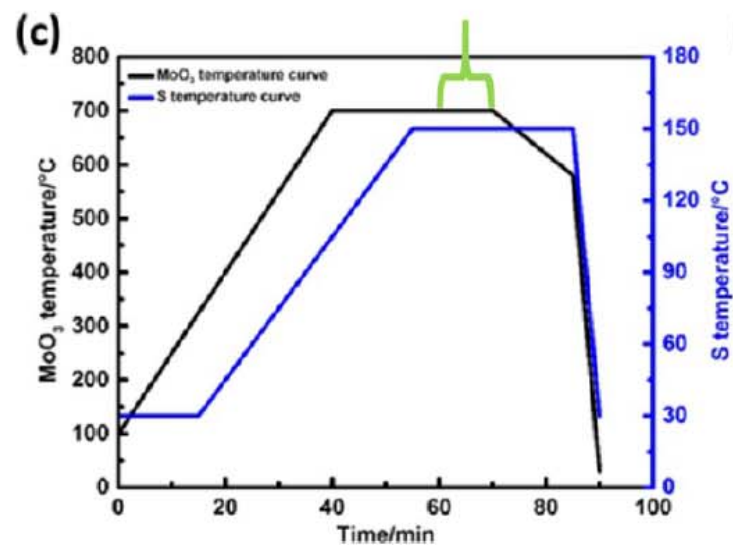
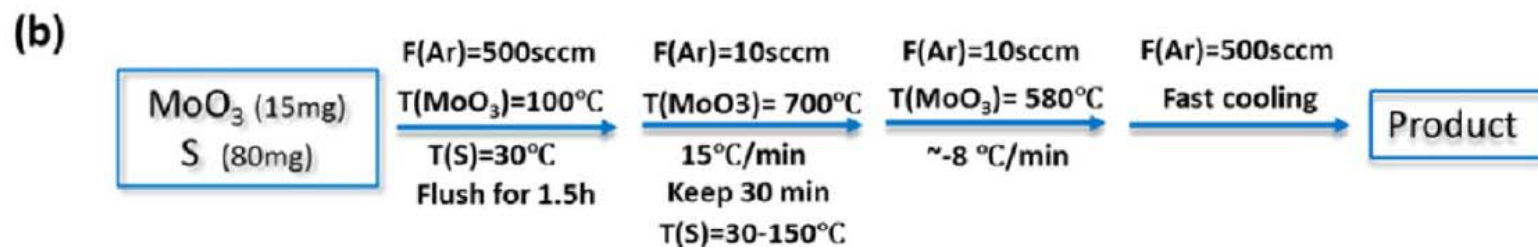
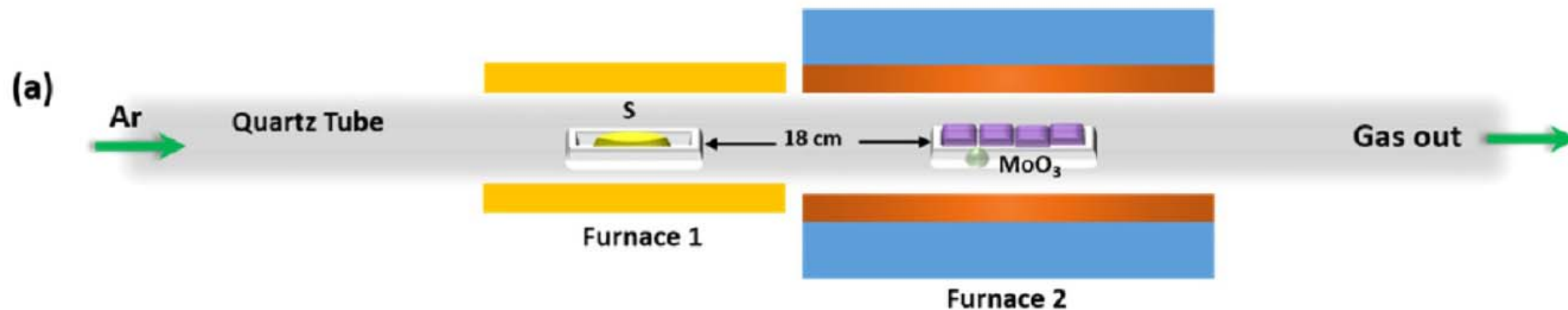
Powder vapor transport (also referred to as chemical vapor deposition)



*M. Chhowalla, et al.
Nature Chemistry 5 (2013) p. 264*

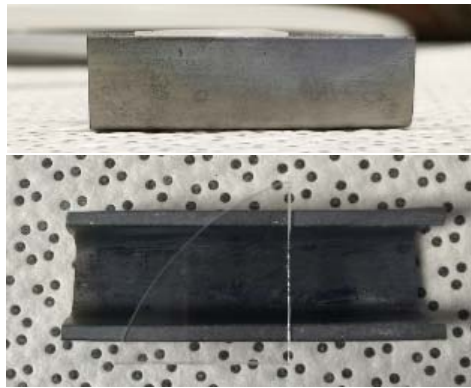
Powder vapor transport

Chem. Mater., 2014, 26 (22), pp 6371-6379

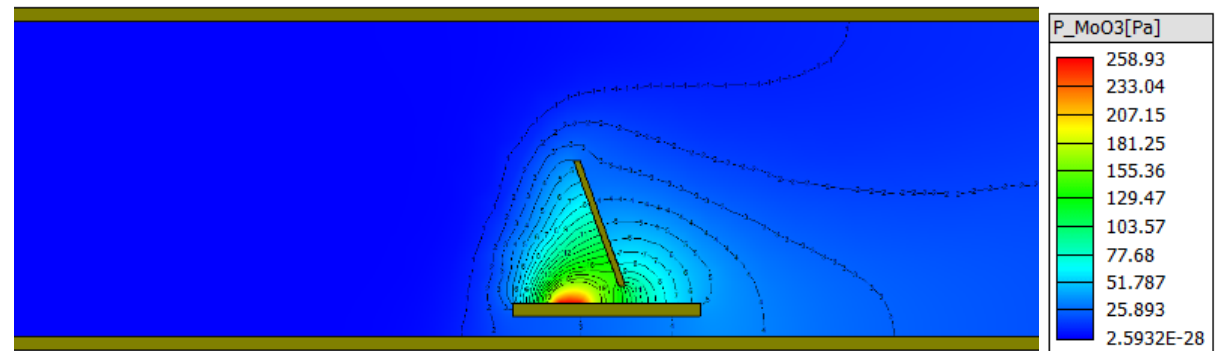
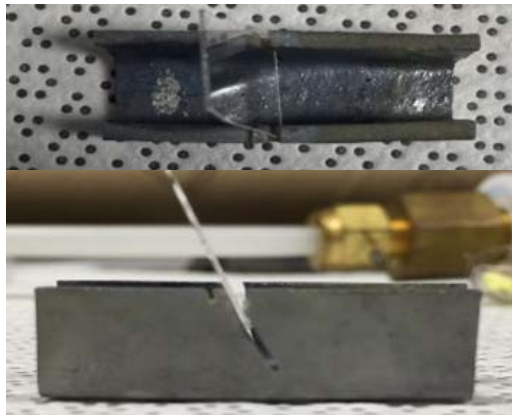
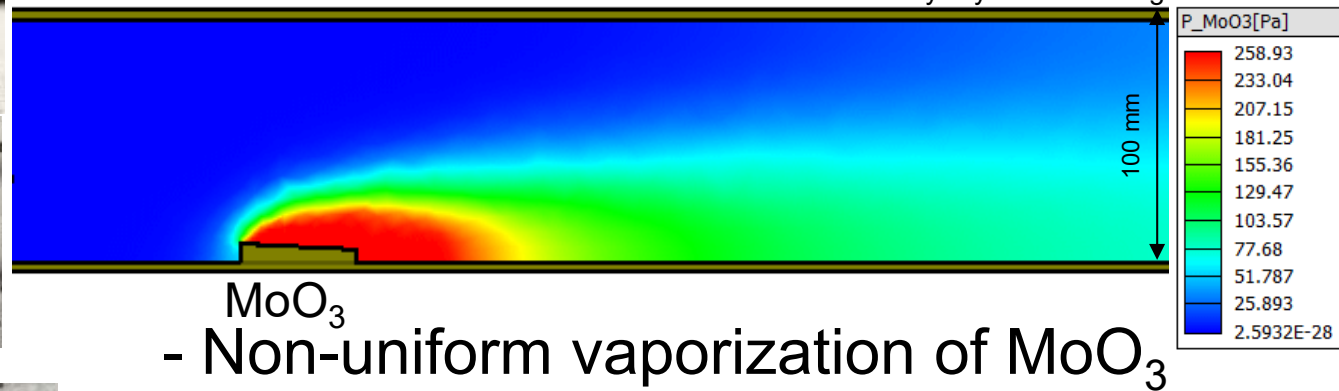


Powder Vaporization

The Case of MoS₂



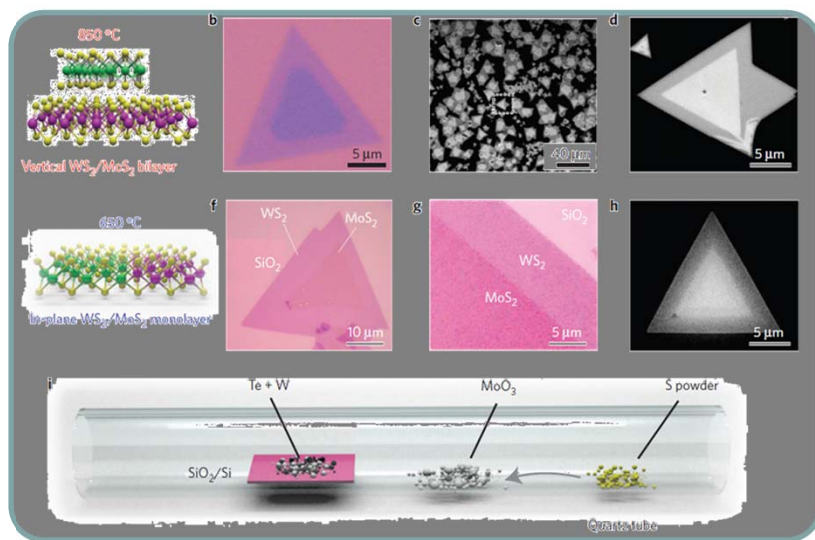
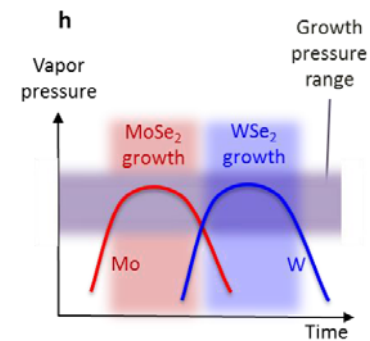
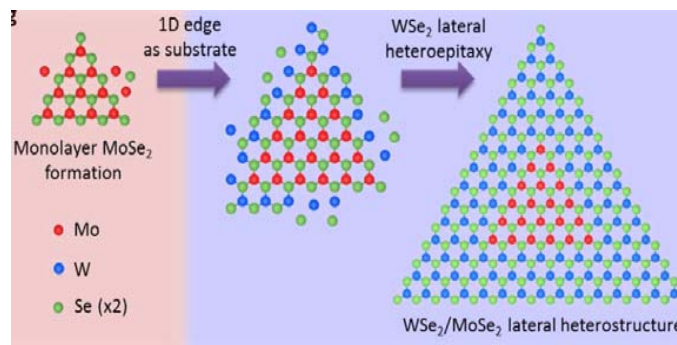
Courtesy: Kyma Technologies



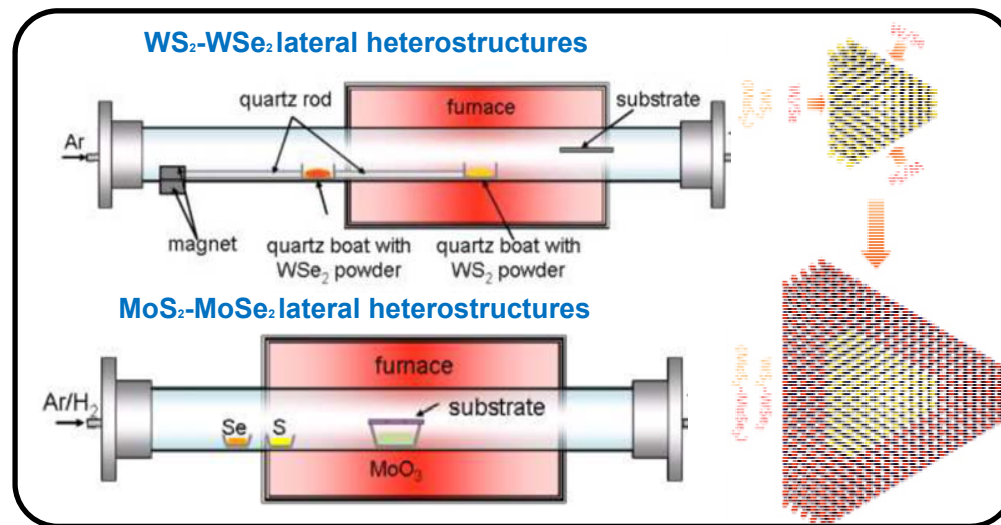
Powder Vapor Transport



Nature Materials, doi:10.1038/nmat4064 (2014)



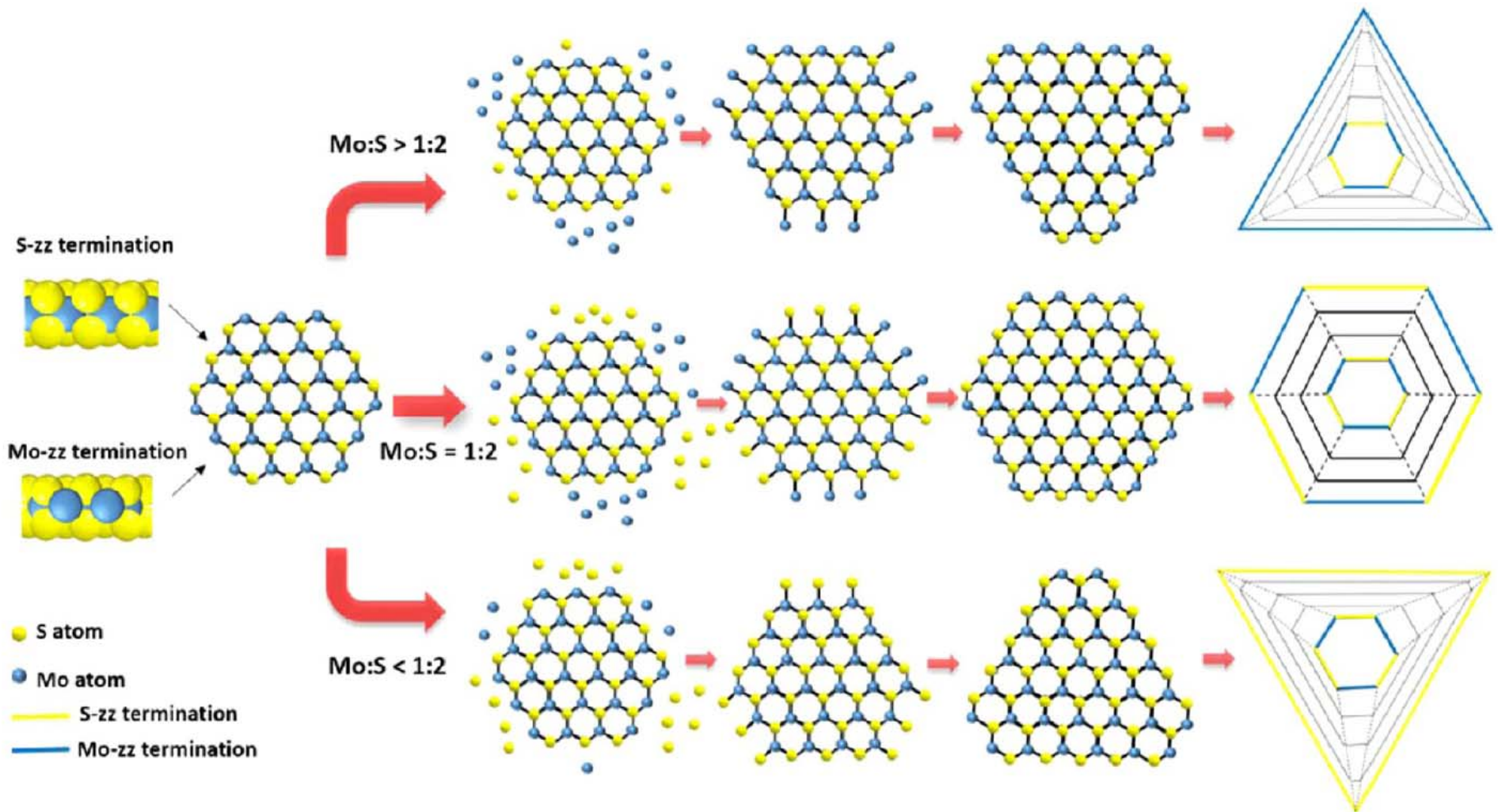
Nature Materials 13, 1135–1142 (2014)



Nature Nanotechnology 9, 1024–1030 (2014)

Powder Vaporization

Chem. Mater., 2014, 26 (22), pp 6371-6379



Point defects

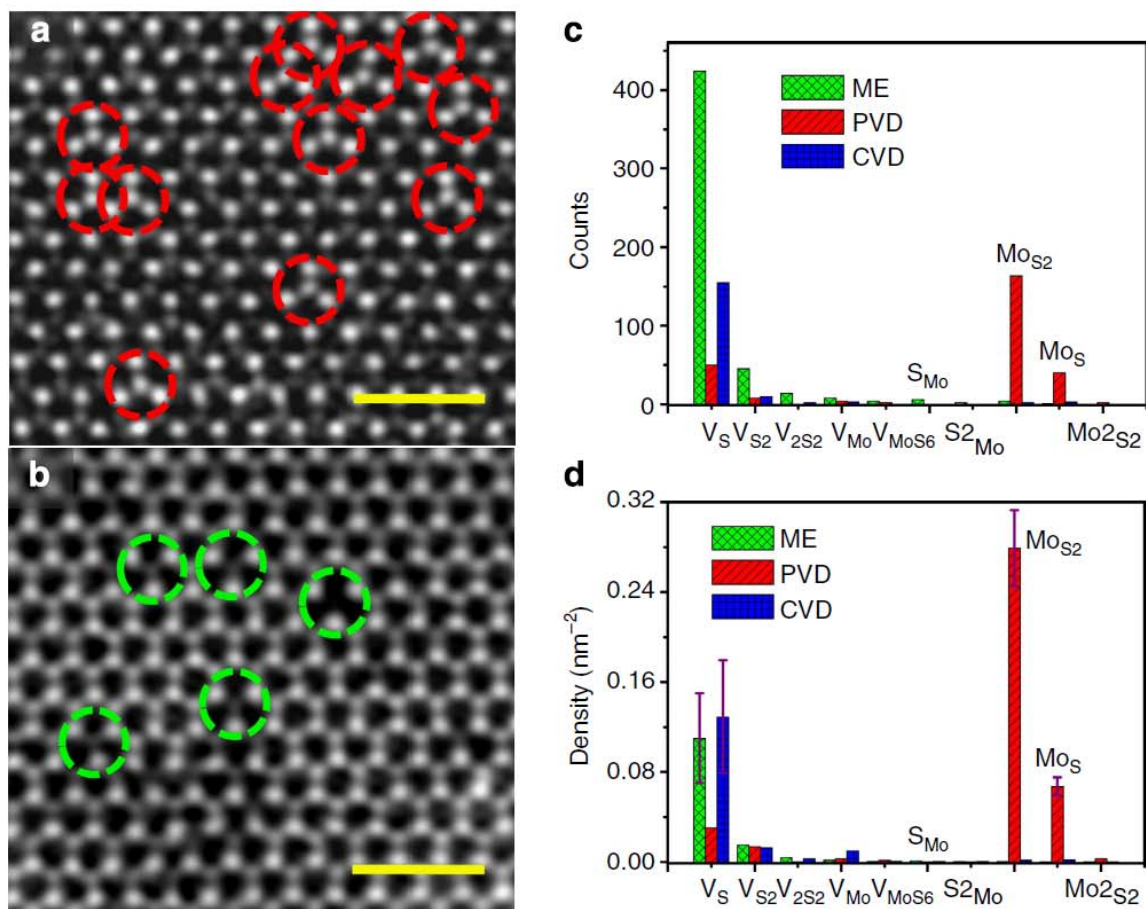
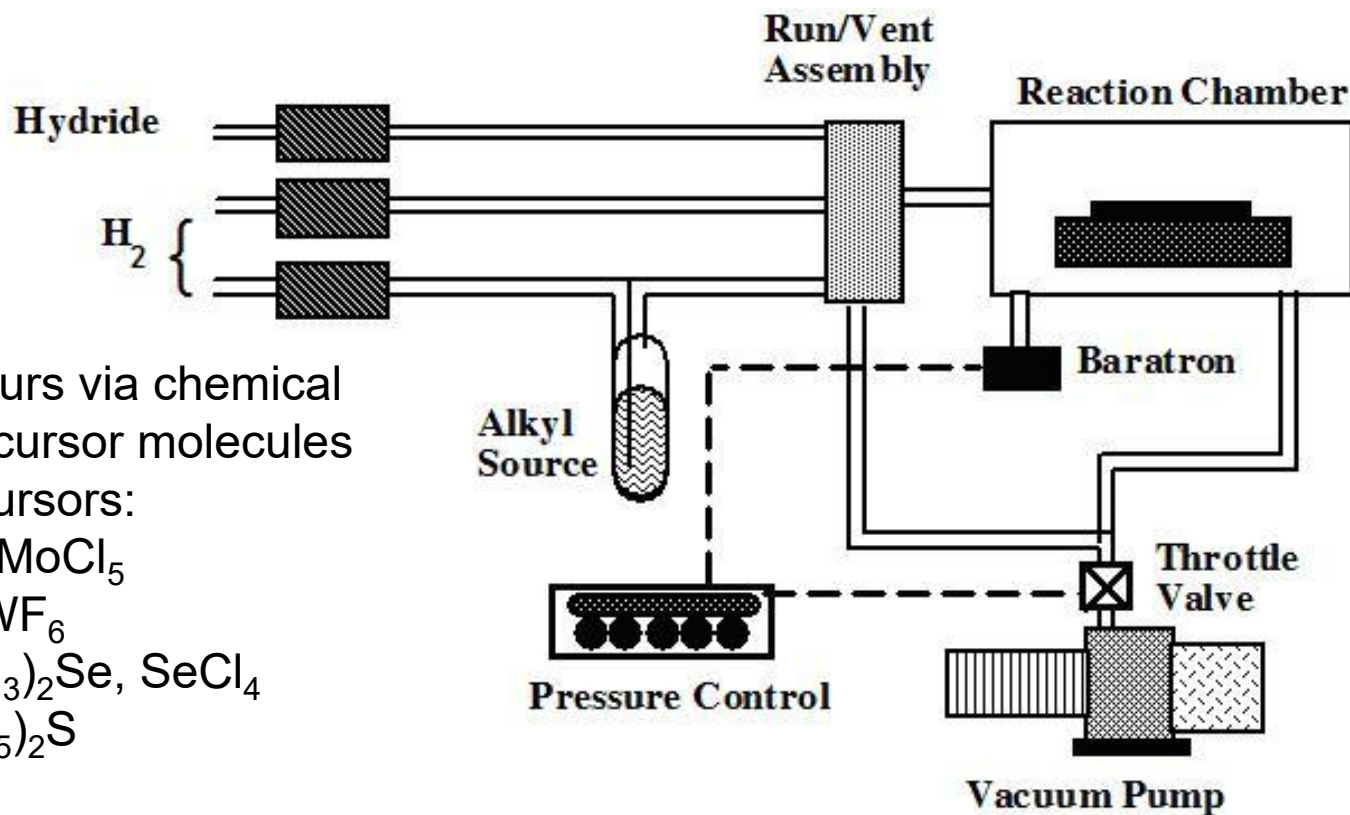


Figure 1 | Atomic resolved STEM-ADF images to reveal the distribution of different point defects. (a) Antisite defects in PVD MoS₂ monolayers. Scale bar, 1 nm. (b) Vacancies including V_S and V_{S2} observed in ME monolayers, similar to that observed for CVD sample. Scale bar, 1 nm. (c,d) Histograms of various point defects in PVD, CVD and ME monolayers. Error estimates are given for the dominant defects (more details on the statistics can be found in Supplementary Fig. 6). ME data are in green, PVD data in red and CVD in blue.

Chemical Vapor Deposition



- Deposition occurs via chemical reaction of precursor molecules
- Variety of precursors:
 - $\text{Mo}(\text{CO})_6$, MoCl_5
 - $\text{W}(\text{CO})_6$, WF_6
 - H_2Se , $(\text{CH}_3)_2\text{Se}$, SeCl_4
 - H_2S , $(\text{C}_2\text{H}_5)_2\text{S}$

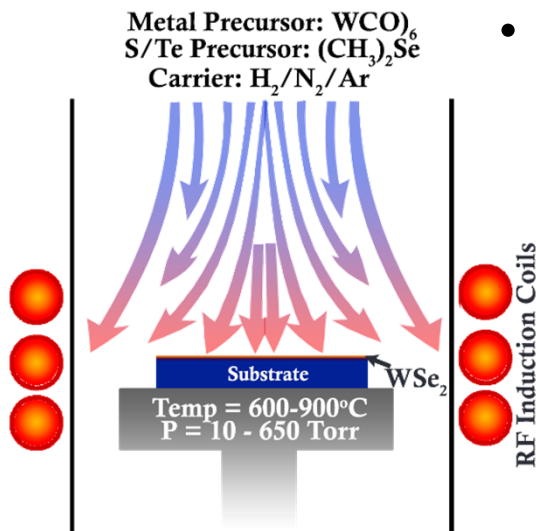
Advantages:

- Scalable to large substrate diameters
- Offers good control over deposition rate
- Can easily change precursors for growth of heterostructures

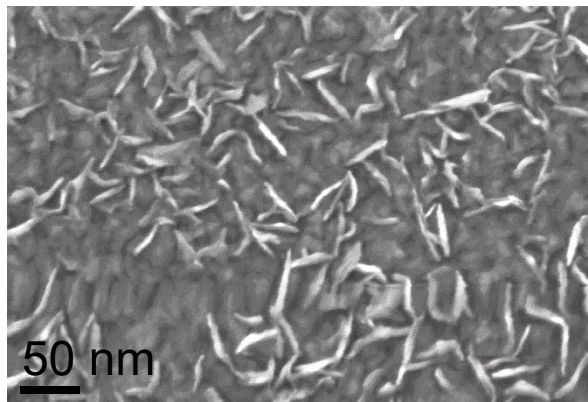
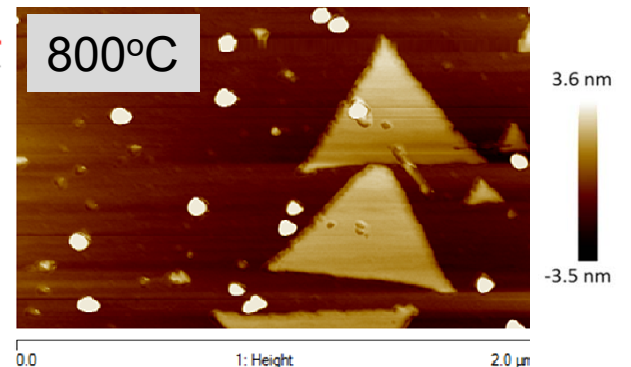
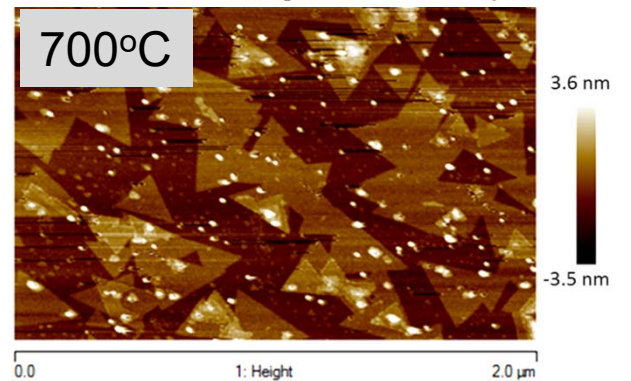
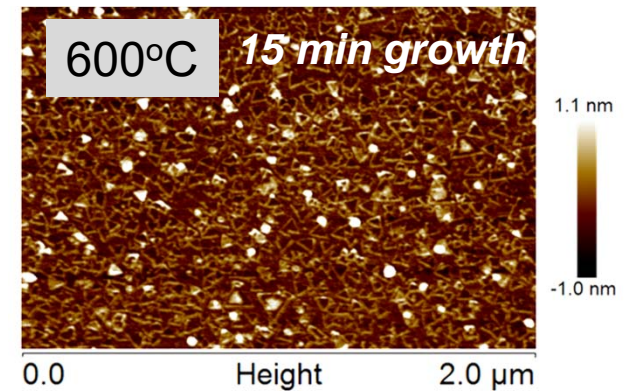
Challenges:

- Mo, W, etc. high melting points ($>2000^\circ\text{C}$)/low vapor pressure
- S, Se, etc. low melting points ($<250^\circ\text{C}$)/high vapor pressure

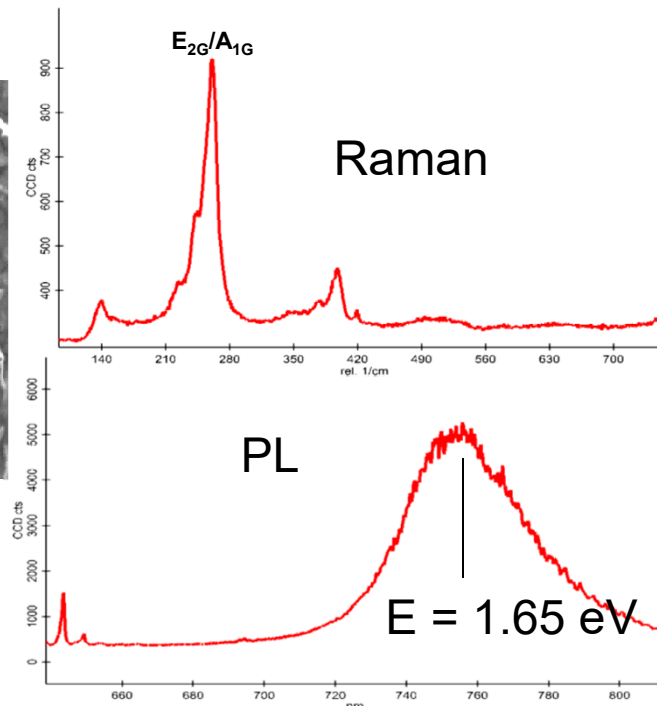
MOCVD of WSe₂



- Very low flow rates of W(CO)₆ required for monolayer growth
- High Pressure (650 Torr)
- 100% Hydrogen ambient
- Raman and PL indicative of monolayer growth



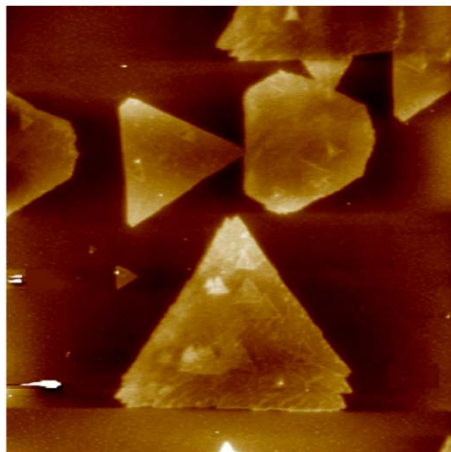
High flow rates of MO precursors leads to thick WSe₂ films, and significant vertical growth



Collaboration with Josh Robinson (PSU MatSE)

MOCVD of WSe₂

c-plane (0001) sapphire



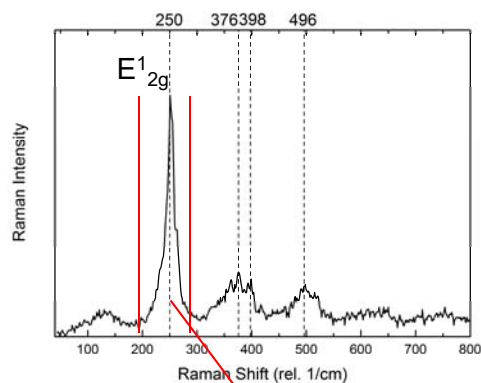
Height

4.0 μm

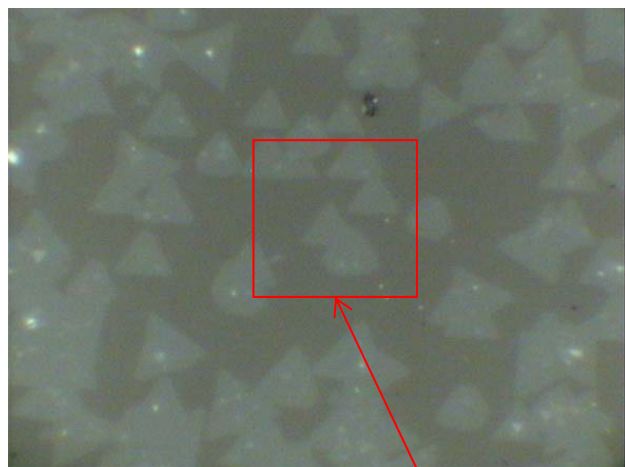
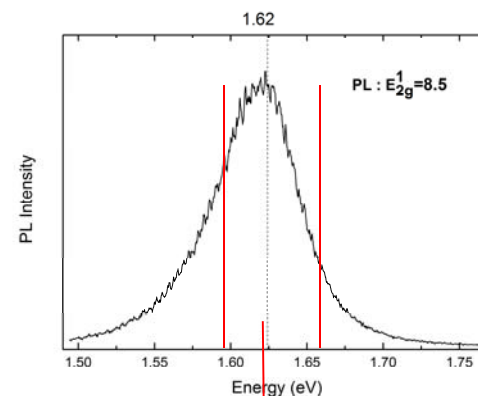
Growth Conditions:

- W(CO)₆, (CH₃)₂Se, H₂ carrier gas
- 800°C, 700 Torr
- W(CO)₆=3.3x10⁻⁴ sccm, Se/W=2.4x10⁵

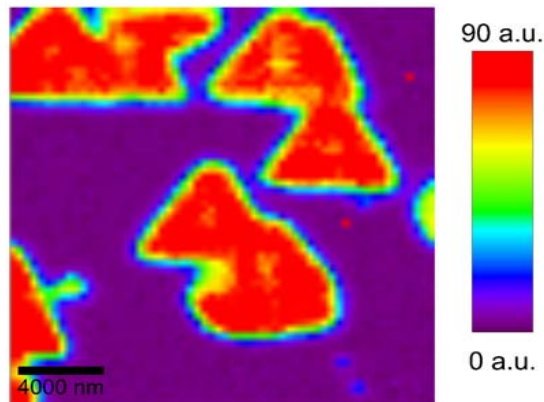
Normalized Raman



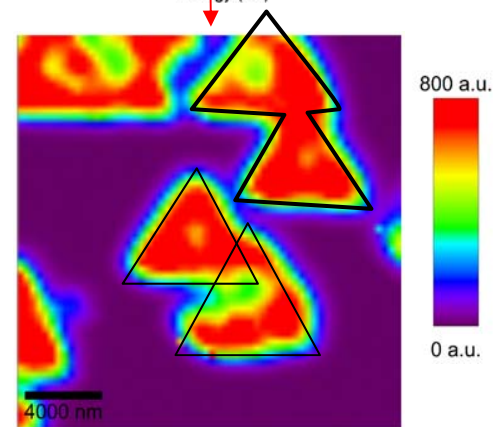
Normalized PL



Mapping region

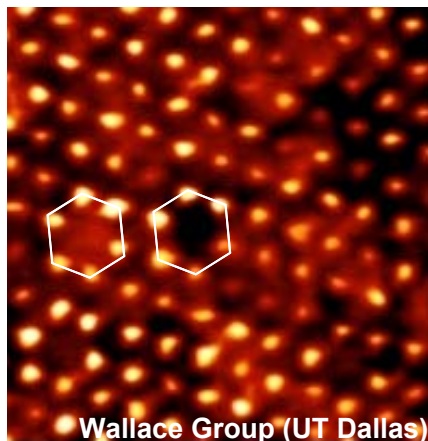


Raman Mapping



PL Mapping 1.60 eV

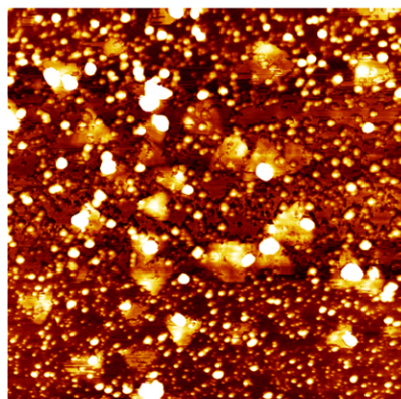
MOCVD of WSe₂: Effect of Se/W Ratio



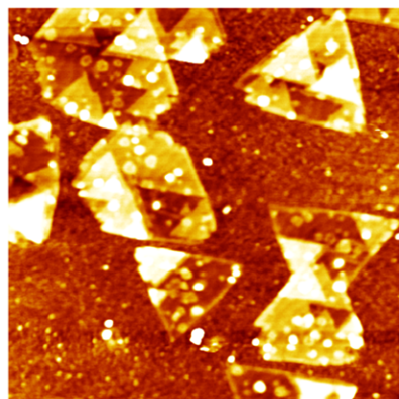
- Defects serve as nucleation sites in 2D materials.
- Typical defects are chalcogen (S, Se, Te) vacancies.

Se:W ratio has significant impact on domain size, shape, and “defect” formation

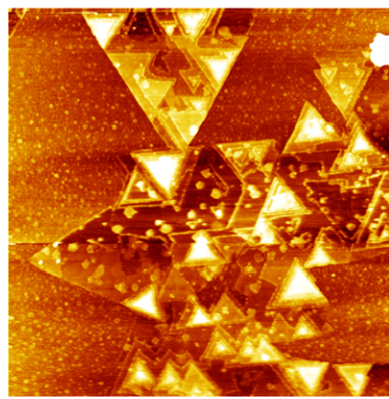
Temp (°C)	Time (min)	Pre- Anneal	Pressure (Torr)
800	30	500C, 15min	700



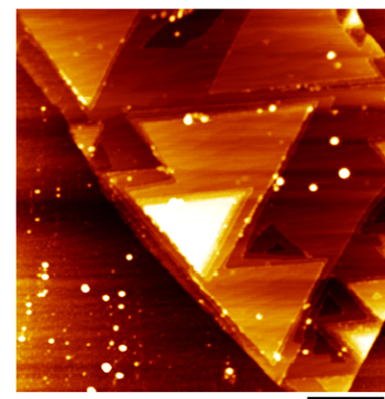
Height 400.0 nm
Se:W Ratio: 170



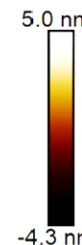
Height 400.0 nm
Se:W Ratio: 400



Height 400.0 nm
Se:W Ratio: 800

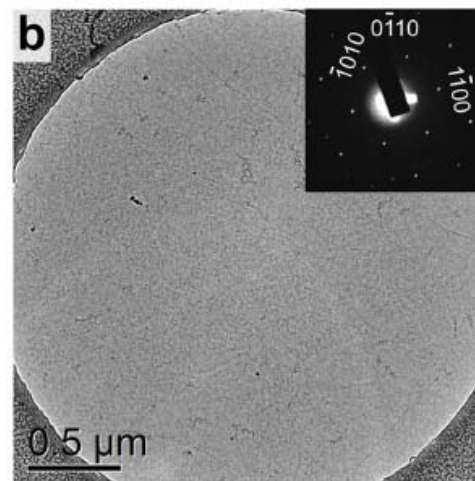
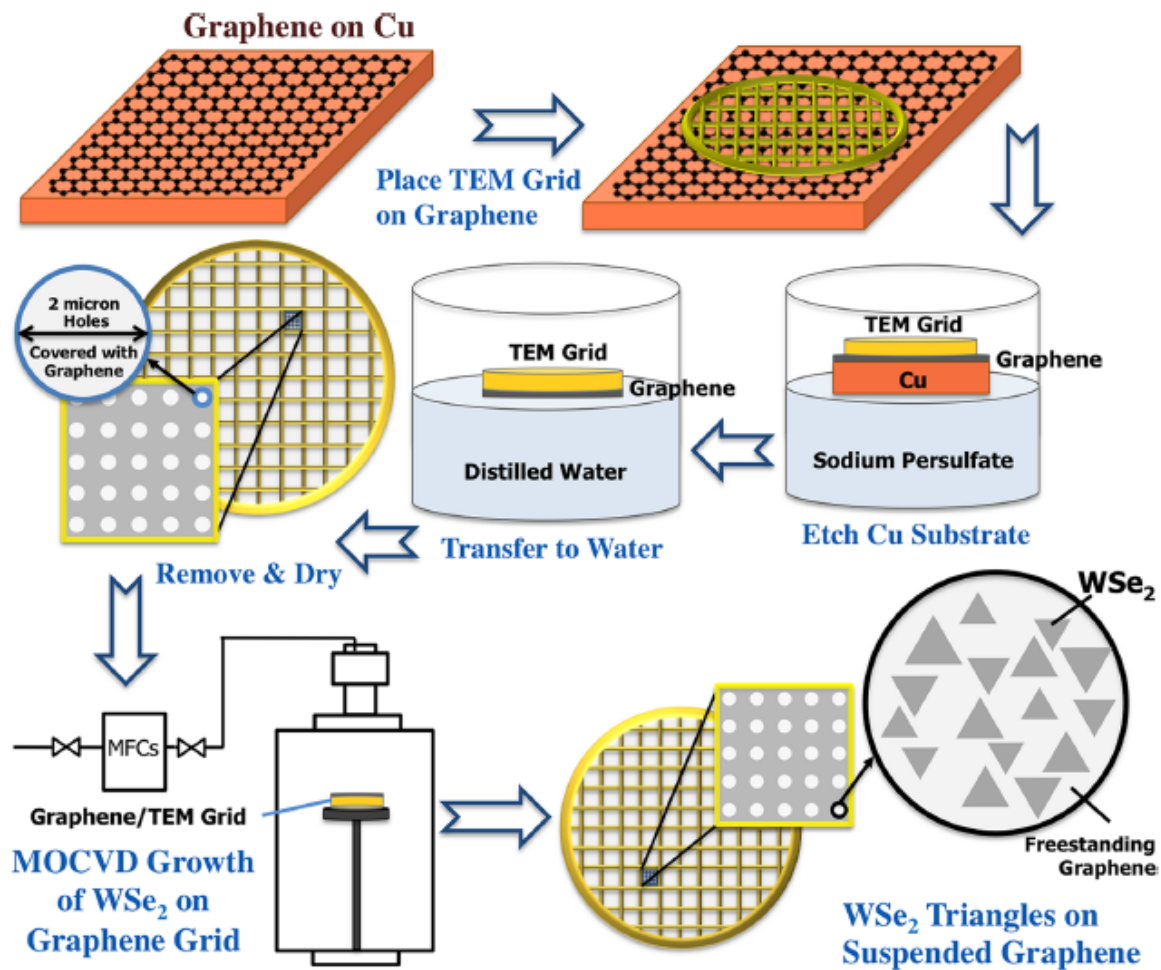


Height 400.0 nm
Se:W Ratio: 14000

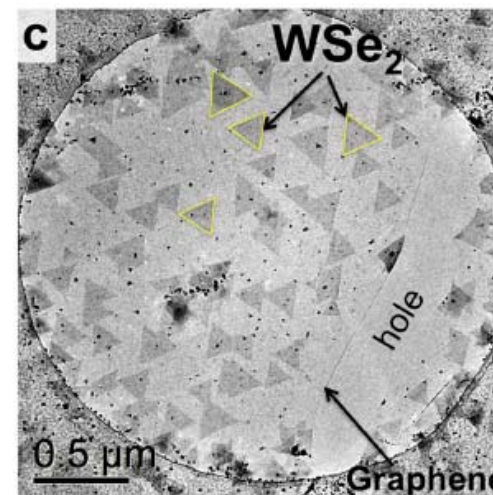


WSe₂ on Free Standing Graphene Templates

Nasim Alem, Josh Robinson



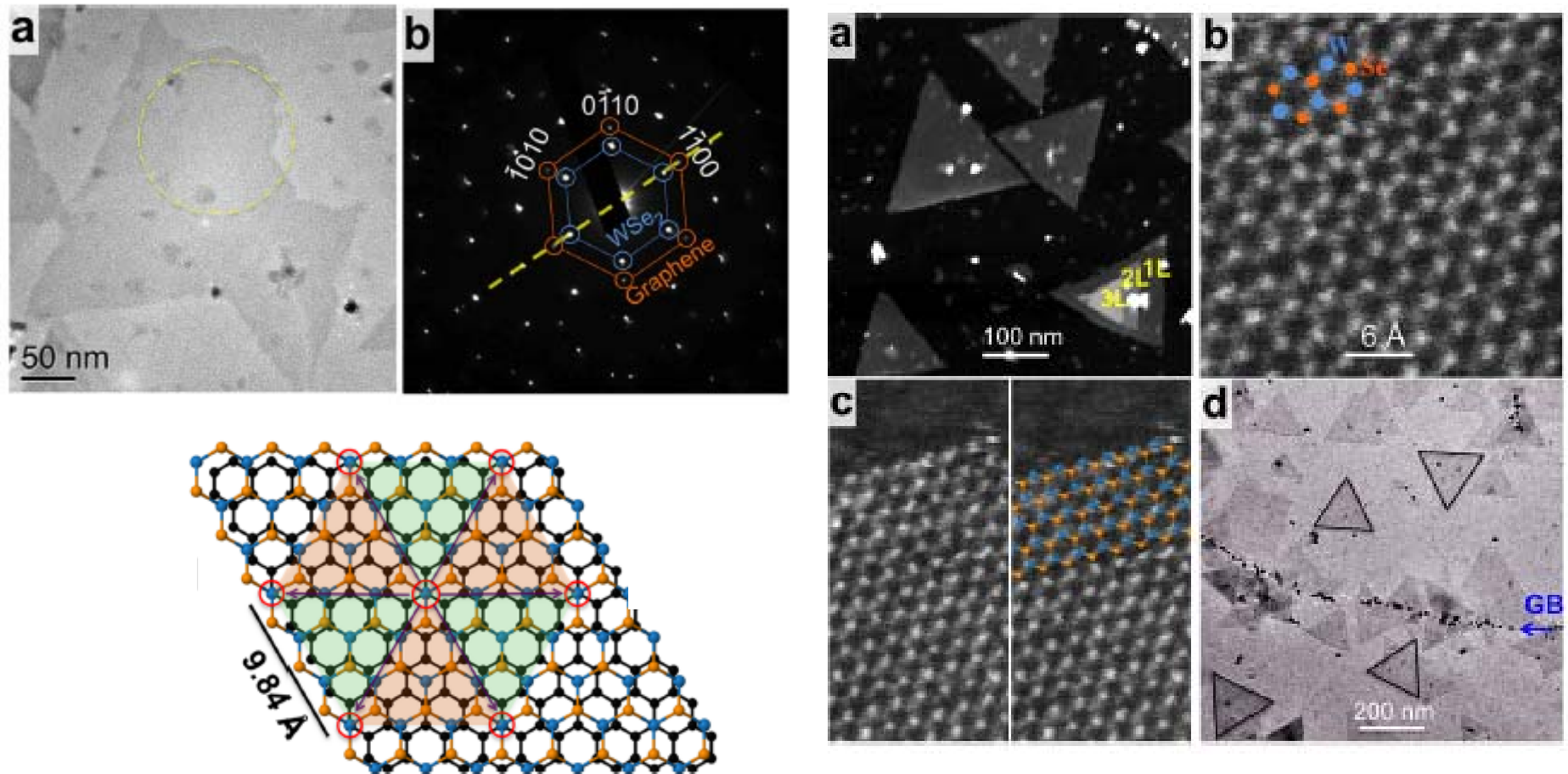
As Prepared



After MOCVD Growth

A. Azizi, et al. ACS Nano (in press)

WSe₂ – Epitaxy and Defects

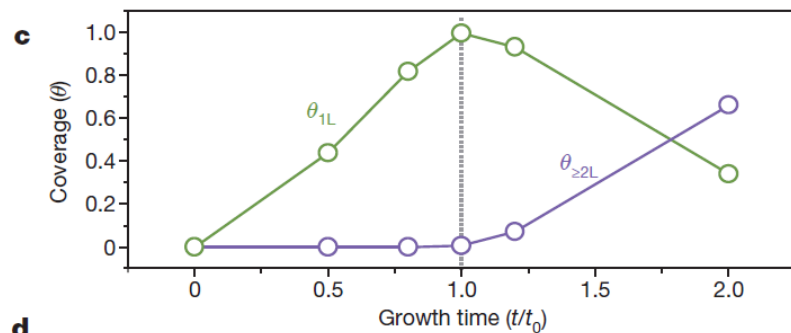
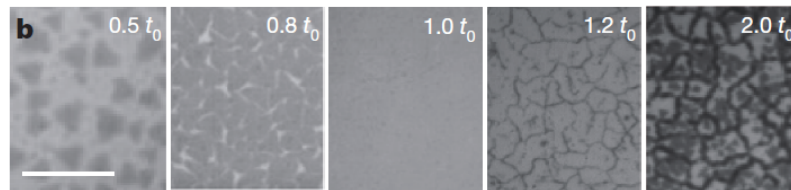
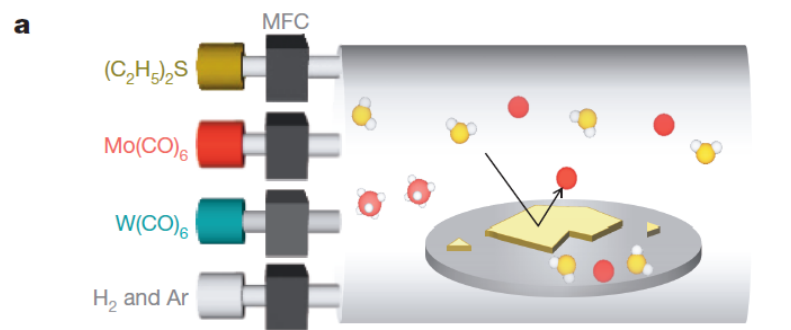


(a) TEM image and (b) SAD pattern showing epitaxial relationship between WSe₂ and graphene
 (c) Structural model showing alignment of W atoms in WSe₂ and C atoms in graphene (circled in red)

(a) HAADF-STEM image of monolayer and multilayer WSe₂
 HAADF-STEM images of (a) monolayer WSe₂ and (b) edge region showing W-termination
 (c) HAADF-STEM image of monolayer WSe₂ and (d) edge region showing W-termination
 (d) TEM image showing nucleation near grain boundary in graphene

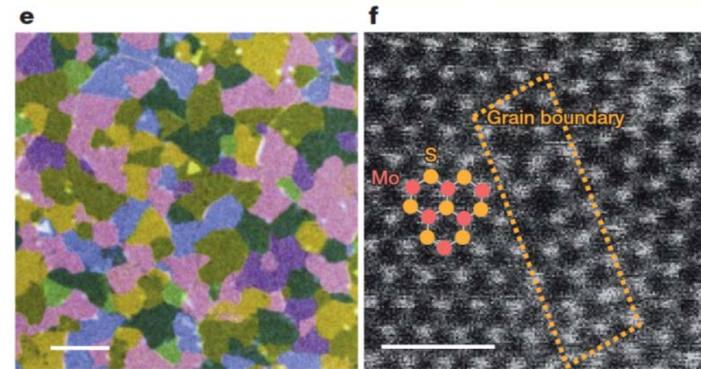
High-mobility three-atom-thick semiconducting films with wafer-scale homogeneity

Kibum Kang^{1*}, Saien Xie^{2*}, Lujie Huang¹, Yimo Han², Pinshane Y. Huang², Kin Fai Mak^{3,4}, Cheol-Joo Kim¹, David Muller^{2,3} & Jiwoong Park^{1,3}



d

$t_0 = 26$ hours



Paper Discussion #2

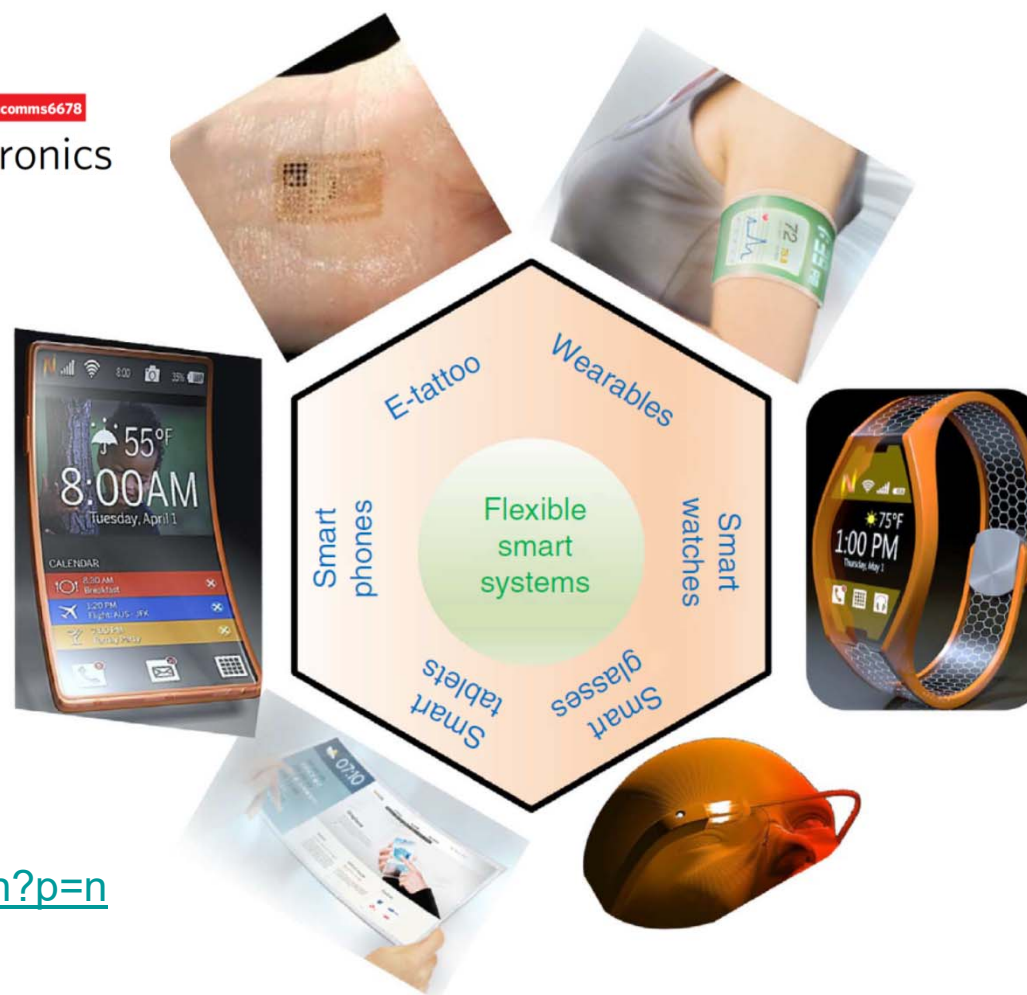
REVIEW

Received 5 Nov 2013 | Accepted 28 Oct 2014 | Published 17 Dec 2014

DOI: 10.1038/ncomms6678

Two-dimensional flexible nanoelectronics

Deji Akinwande¹, Nicholas Petrone² & James Hone²

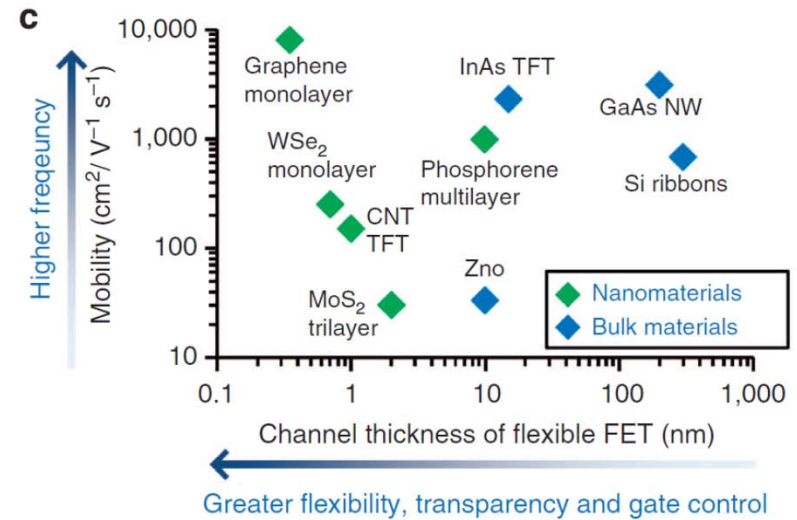
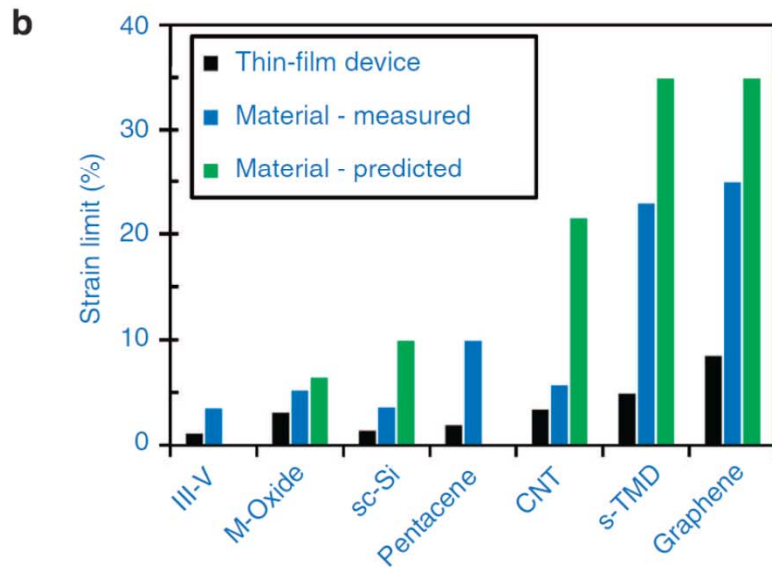
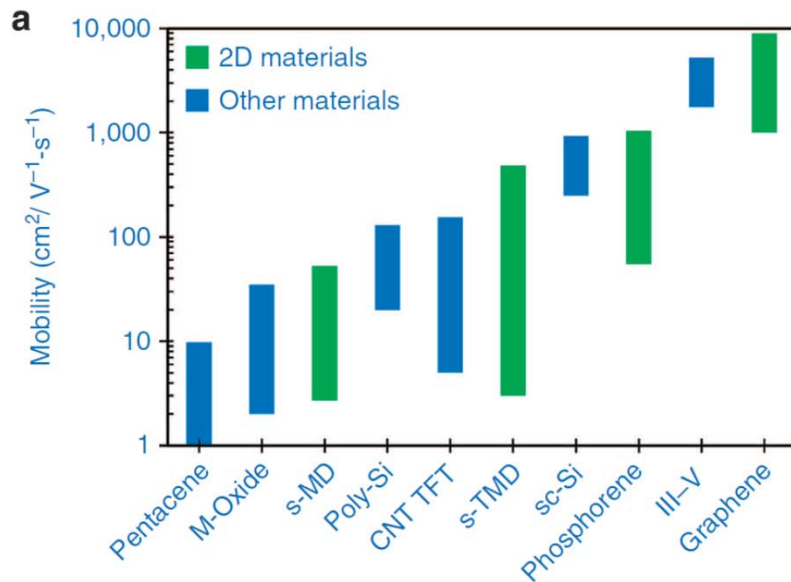


Watch Nokia Morph video:

<https://search.yahoo.com/yhs/search?p=nokia+morph+video&ei=UTF-8&hspart=moz>

What properties are important for flexible electronics?

Why 2D materials?



Properties of selected 2D materials

Table 1 | Room temperature solid-state properties of selected 2D crystalline materials.

2D Material	Optical		Electrical		Mechanical		Thermal		References
	Band gap (eV)	Band Type	Device Mobility ($\text{cm}^2 \text{V}^{-1} \text{s}^{-1}$)	v_{sat} (cm s^{-1})	Young's Mod. (GPa)	Fracture strain (%) Theor (Meas)	κ ($\text{W m}^{-1} \text{K}^{-1}$)	CTE (10^{-6}K^{-1})	
Graphene	0	D	10^3 - 5×10^4	1 - 5×10^7	1,000	27-38 (25)	600-5,000	- 8	4-11
1L MoS ₂	1.8	D	10-130	4×10^6	270	25-33 (23)	40	NA	1,19-21,27,92
Bulk MoS ₂	1.2	I	30-500	3×10^6	240	NA	50 (), 4 (\perp)	1.9 ()	1,15,62,92-95
1L WSe ₂	1.7	D	140-250	4×10^6	195	26-37 (NA)	NA	NA	1,16,84,96
Bulk WSe ₂	1.2	I	500	NA	75-100	NA	9.7 (), 2 (\perp)	11 ()	1,93,97-100
h-BN	5.9	D	NA	NA	220-880	24 (3-4)	250-360 () 2 (\perp)	- 2.7	22-25
Phosphorene	0.3-2*	D	50-1,000	NA	35-165	24-32	10-35 ()	NA	28-30

h-BN, hexagonal boron nitride; NA, not available; 2D, two-dimensional.

All listed values should be considered estimates. In some cases, experimental or theoretical values are not available (NA).

*The precise value for the bandgap, which is a maximum for a monolayer is a matter of ongoing research.

The || symbol signifies the in-plane direction; \perp signifies the out of plane direction.

2D Thin Film Transistors

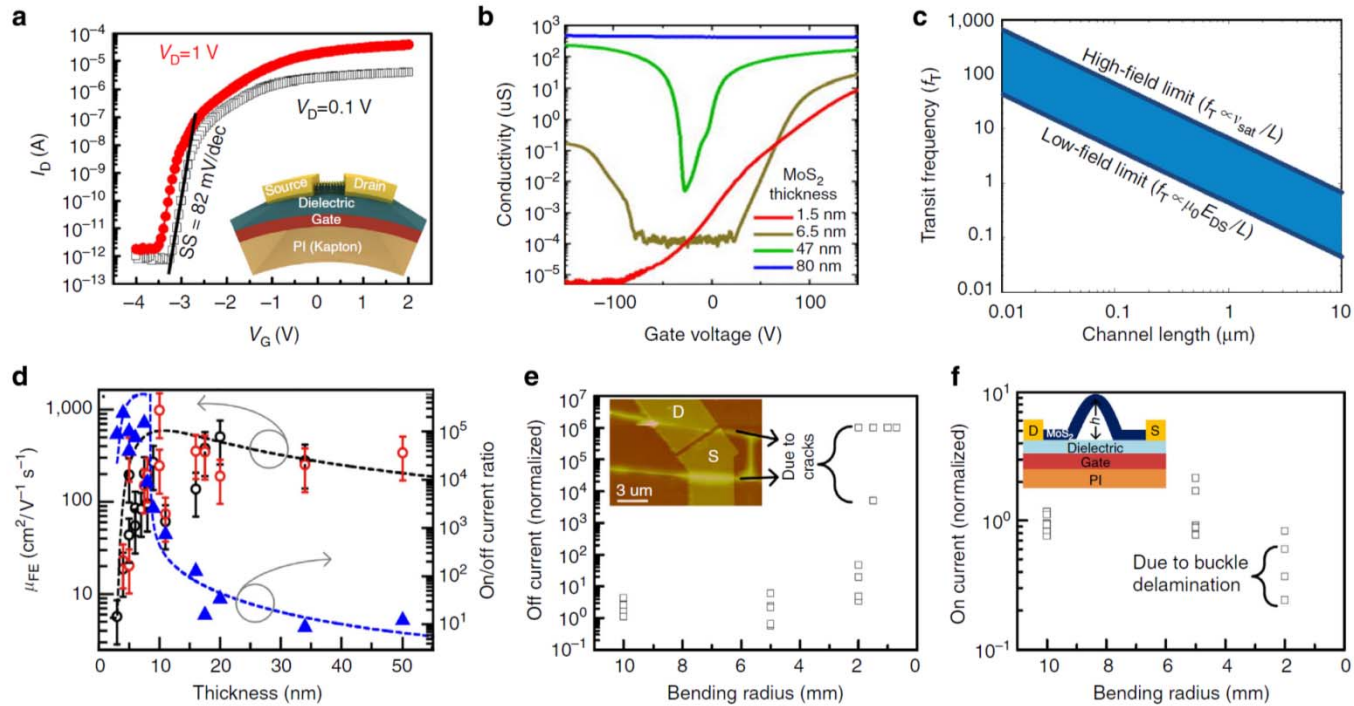


Figure 4 | High-performance room-temperature 2D TFTs. (a) Transfer characteristics of a multilayer MoS₂ FET ($W/L = 3/1\mu\text{m}$) with high- k gate dielectric featuring an on/off switching ratio $>10^7$ and sub-threshold slope (SS) of ~ 82 mV per decade fairly close to the ideal limit of 60 mV per decade. Inset is a schematic of the flexible device. (Adapted, with permission, from ref. 17 (copyright 2013 American Chemical Society).) (b) Conductivity as a function of gate voltage for four MoS₂ devices on PMMA surfaces. The peak field-effect mobilities are 30, 68 and 480 $\text{cm}^2\text{V}^{-1}\text{s}^{-1}$, corresponding to MoS₂ thicknesses of 1.5, 6.5 and 47 nm, respectively. Reproduced, with permission, from ref. 62 (copyright 2013, AIP Publishing LLC). (c) Estimated (intrinsic) transit frequency of TMDs based on equation (1) and constant-field channel length scaling. The low- and high-field limits are determined by the low-field mobility ($\mu_0 \sim 30 \text{ cm}^2\text{V}^{-1}\text{s}^{-1}$, $f_T L \sim 0.4 \text{ GHz}\cdot\mu\text{m}$) and saturation velocity ($v_{\text{sat}} \sim 4 \times 10^6 \text{ cm s}^{-1}$, $f_T L \sim 6 \text{ GHz}\cdot\mu\text{m}$) respectively. (d) Reported carrier mobility (four-terminal, black circles; two-terminal, red circles) and drain current modulation (blue triangles) of phosphorene FETs of varying thicknesses. The dashed lines are derived from modelling. (Adapted from ref. 28.) (e) Mechanical studies of flexible MoS₂ FETs. Below 2 mm bending radius, the exponential increase in off current is due to cracks in the gate dielectric shown in the inset. (f) Similarly, the on current degrades, but primarily owing to buckling delamination, which is thickness dependent. Inset is an illustration of device buckling. (e,f) © 2013 IEEE. Reproduced, with permission, from ref. 58.

Heterostructure devices

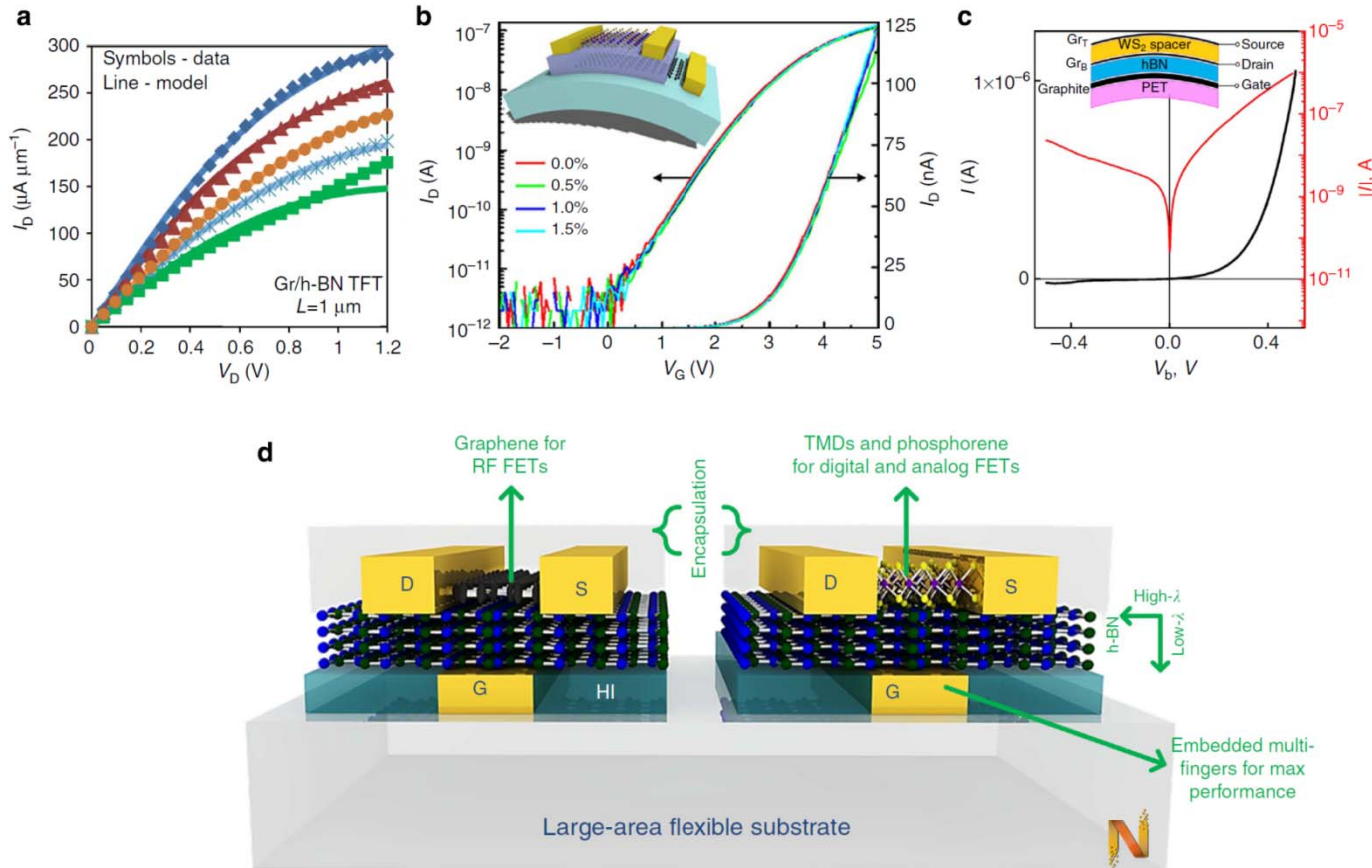


Figure 5 | Flexible 2D heterostructure devices. (a) Output characteristics of a TFT consisting of a graphene/h-BN channel/dielectric heterostructure stack on PI substrate showing soft current saturation and high current density. Gr: graphene. (© 2013 IEEE. Reproduced, with permission, from ref. 39.) (b) Transfer curves of a transparent trilayer TFT with a MoS₂ channel, h-BN gate dielectric and few-layer graphene gate electrode on PEN substrate featuring robust electronic properties under different bending conditions up to 1.5% strain. The inset shows the schematic diagram of the flexible device. Adapted, with permission, from ref. 18 (copyright 2013 American Chemical Society). (c) Room-temperature tunnel current of a five-layer flexible heterostructure vertical tunnel transistor. The data shown are at zero gate voltage and 20 mm bending radius. WS₂ thickness is around 3-10 layers. Schematic of the vertical transistor is shown in the inset. (Adapted from ref. 66.) (d) Simplified illustration of the proposed ideal integrated heterogeneous flexible device structure, which employs graphene for RF electronics and semiconducting TMDs or phosphorene for low-power complementary digital and analogue devices. h-BN is ideal as a multifunctional gate dielectric for mobility enhancement, high velocity saturation and thermal management of the channel heat based on its desirable anisotropic thermal conductivity (λ). A hydrophobic coating can preserve device performance. The embedded back-gate process can enable multiple gate fingers, low gate resistance and high current density. HI refers to an heat insulator.

Roll-to-roll manufacturing

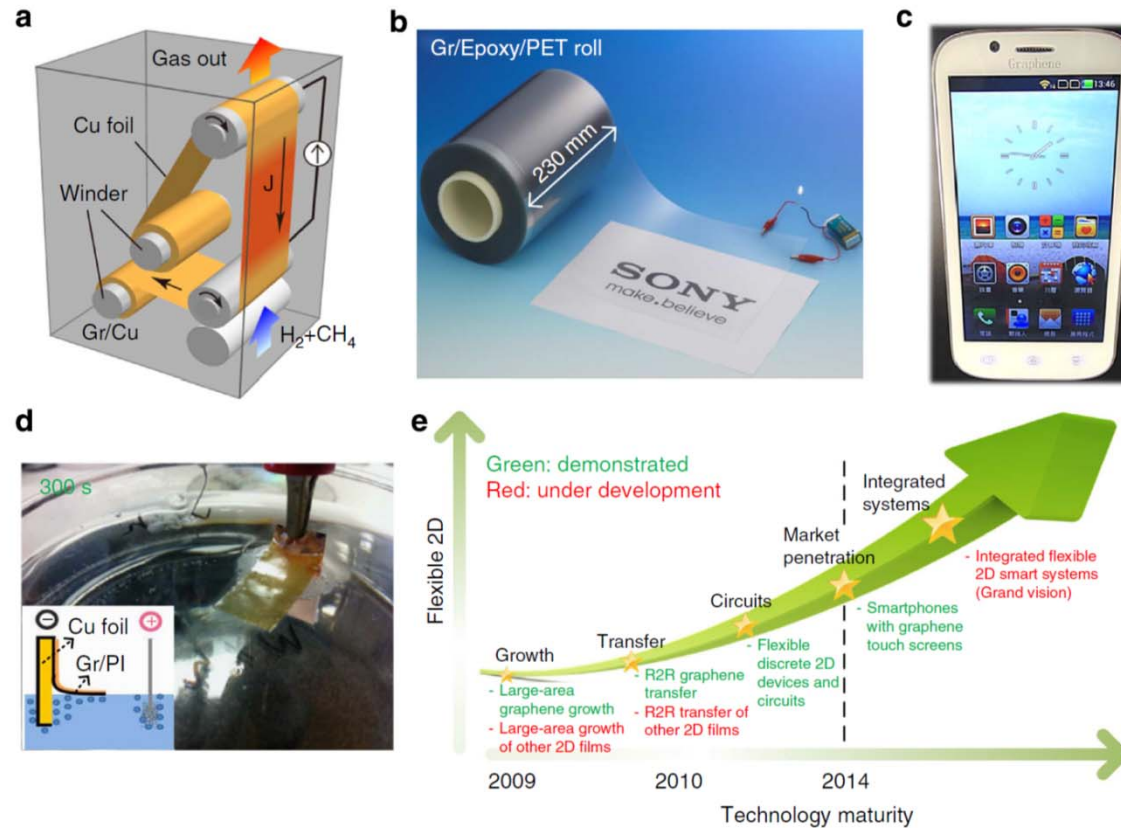


Figure 7 | Large-scale nanomanufacturing. (a) A scheme for continuous R2R growth of graphene based on selective Joule heating of copper foil. Gr: graphene. (b) The growth is followed by R2R coating and bonding to PET, and finally, the spray etching of the copper substrate to manufacture 100 m long transparent conductive graphene/plastic rolls. (c) Large-scale manufacturing of graphene has enabled smart phones with graphene touch screens, which are now sold in China (Image courtesy of 2D Carbon Tech). (d) Experimental demonstration of electrochemically delaminated graphene onto PI that affords reuse of Cu foil for a sustainable nanomanufacturing technology. Inset is an illustration of the electrochemical method. Reproduced, with permission, from ref. 74 (© 2013 WILEY-VCH Verlag & Co. KGaA, Weinheim). (e) Simplified technology maturity perspective for flexible 2D nanotechnology. Growth, transfer and circuits based on graphene have been demonstrated leading to the 2013–2014 market penetration of graphene as smart phone touch panels. The large-scale advancement of graphene is expected to benefit the progress of other 2D sheets, and graphene’s market penetration can be a launch pad for the commercial development of fully integrated flexible smart systems using 2D materials for both passive and active devices. (a,b) Reproduced with permission from ref. 73. (copyright 2013, AIP Publishing LLC).